

NUREG/CR-1945
LA-8703-MS



**Sensitivity of Slab Core Test Facility
Calculational Model Execution to
Certain TRAC Input Parameters**

University of California



LOS ALAMOS SCIENTIFIC LABORATORY

Post Office Box 1663 Los Alamos, New Mexico 87545

8107100332 810630
PDR NUREG
CR-1945 R PDR

An Affirmative Action/Equal Opportunity Employer

NOTICE

This report was prepared as an account of work sponsored by an agency of the United States Government. Neither the United States Government nor any agency thereof, or any of their employees, makes any warranty, expressed or implied, or assumes any legal liability or responsibility for any third party's use, or the results of such use, of any information, apparatus, product or process disclosed in this report, or represents that its use by such third party would not infringe privately owned rights.

NUREG/CR-1945
LA-8703-MS
R4

Sensitivity of Slab Core Test Facility Calculational Model Execution to Certain TRAC Input Parameters

Suzanne T. Smith

Manuscript submitted: January 1981
Date published: June 1981

Prepared for
Division of Reactor Safety Research
Office of Nuclear Regulatory Research
US Nuclear Regulatory Commission
Washington, DC 20555

NRC FIN No. A7049



UNITED STATES
DEPARTMENT OF ENERGY
CONTRACT W-7405-ENG. 36

SENSITIVITY OF SLAB CORE TEST FACILITY
CALCULATIONAL MODEL EXECUTION TO
CERTAIN TRAC INPUT PARAMETERS

by

Suzanne T. Smith

ABSTRACT

Statistical correlation methods have been used to determine the sensitivity of the TRAC model for the Slab Core Test Facility to certain TRAC input parameters in order to optimize the calculations projected for FY 1981. By means of nonparametric statistical methods, it has been determined that reasonable convergence for minimum running time can be attained with a specific set of input timing and convergence criteria, thus effecting a savings in the anticipated cost of these calculations.

I. INTRODUCTION

The 2D-3D Program is a multinational analysis and experimental program to study detailed multidimensional behavior of the major subsystems of a nuclear power plant during a postulated loss-of-coolant accident sequence. The Federal Republic of Germany has built and is operating the Primary Coolant Loop Test Facility (PKL) and will build and operate the Upper Plenum Test Facility (UPTF). The Japan Atomic Energy Research Institute (JAERI) has built and is operating two of the test facilities: the Cylindrical Core Test Facility (CCTF), a full-height, one-fifth radial scale electrically heated facility, and the Slab Core Test Facility (SCTF), a full-height, eight-bundle-wide electrically heated slab facility. The Los Alamos National Laboratory, through

support of the United States Nuclear Regulatory Commission (USNRC), is responsible for the analysis support and for some of the instrumentation design and fabrication.

The analysis tool used is the Transient Reactor Analysis Code (TRAC)¹ being developed at the Los Alamos National Laboratory to provide an advanced "best estimate" predictive capability for the analysis of postulated accidents in light water reactors. TRAC provides this analysis capability for pressurized water reactors (PWRs) and for a wide variety of thermal-hydraulic experimental facilities. It features a three-dimensional treatment of the pressure vessel and associated internals; one-dimensional loop component models; two-phase nonequilibrium hydrodynamics models; flow-regime-dependent constitutive equation treatment; reflood tracking capability for both bottom flood and falling film quench fronts; and consistent treatment of entire accident sequences including the generation of consistent initial conditions.

The purpose of the SCTF experiments is to provide insight into the thermal-hydraulic behavior of a PWR during the end-of-blowdown, refill and reflood phases of a hypothetical loss-of-coolant accident (LOCA) sequence. Of particular interest are core radial flow distributions, liquid entrainment in the core and carryover into the upper plenum, upper plenum liquid pool formation and fallback into the core, quench front propagation, condensation effects, emergency core cooling performance, and overall refill and reflood behavior.

The SCTF designers intended the slab to simulate a radial slice of a typical PWR from its center through the vessel wall. The typical PWR is intended to be either the 15 x 15 Westinghouse/Japanese reference PWR or the 16 x 16 German PWR. The SCTF Core I design is a compromise between these two reference PWRs; the number of spacers and axial lengths will simulate the Westinghouse/Japanese reactor, while the horizontal width will represent the Kraftwerk Union (KWU) German PWR design.

The facility is composed of the pressure vessel, primary coolant system, emergency core cooling (ECC) system, and two containment tanks. The pressure vessel contains the core, downcomer, upper and lower plena, barrel baffle

region, and upper head. The primary coolant system comprises an intact loop, a broken loop with valves to simulate breaks, a steam-water separator, and a pump simulator. ECC water can be injected into the cold leg between the vessel and the steam-water separator and through four injection ports directly into the upper plenum above the tie-plate.

With the SCTF nearing completion and the first tests scheduled to begin in early 1981, the TRAC¹ calculational model of the facility is being streamlined. Because the first reflood calculation² took eighteen hours of CDC-7600 CPU time, it seemed wise to attempt to optimize the execution time with respect to certain input timing and convergence criteria.

During the past few years, methods have been developed at the Los Alamos National Laboratory for studying the sensitivity of output parameters of large computer codes to sets of input parameters.³ These methods require relatively few calculations to achieve meaningful statistical results. The basis for the methods was developed by Kendall⁴ some decades ago; a good background can be found in Ref. 5.

II. SUMMARY OF THE METHOD

A number of input variables that may affect any or all of the set of output parameters to be investigated is first chosen. A range of values is then selected for the input variables. The required number of calculations is determined by the minimum number of mutually independent (in the statistical sense) sets of these variables resulting in a quantile of the Kendall test statistic less than or equal to the 90.0 percentile. Table I shows the quantiles for the Kendall test statistic.

An initializing computer program based on these methods, written at the Los Alamos National Laboratory, was used in determining the statistical independence of the input variables selected for this study. The method assumes a bivariate random sample of size n ; the input variables are then examined in pairs, with N_c tabulated as the number of concordant pairs (defined as all members of one observation larger than the corresponding members of another observation) and N_d tabulated as the number of discordant pairs (when

TABLE I. UPPER QUANTILES FOR THE KENDALL TEST STATISTIC

<i>n</i>	<i>p</i> = .900	.950	.975	.990	.995
4	4	4	6	6	6
5	6	6	8	8	10
6	7	9	11	11	13
7	9	11	13	15	17
8	10	14	16	18	20
9	12	16	18	22	24
10	15	19	21	25	27
11	17	21	25	29	31
12	18	24	28	34	36
13	22	26	32	38	42
14	23	31	35	41	45
15	27	33	39	47	51
16	28	36	44	50	56
17	32	40	48	56	62
18	35	43	51	61	67
19	37	47	55	65	73
20	40	50	60	70	78
21	42	54	64	76	84
22	45	59	69	81	89
23	49	63	73	87	97
24	52	66	78	92	102
25	56	70	84	98	108
26	59	75	89	105	115
27	61	79	93	111	123
28	66	84	98	116	128
29	68	88	104	124	136
30	73	93	109	129	143

one member might be larger and another might be smaller than the corresponding members of another observation). To test the hypothesis of mutual independence, Kendall's test statistic is given as

$$T = N_c - N_d, \tag{1}$$

which is then looked up in Table I. If the value of T exceeds the quantile for the required confidence level and number of observations, the hypothesis is rejected (that is, the set is not mutually independent).

Once the minimum number of calculations has been determined, the computer code in question is run for the predetermined time and each of the selected output parameters is plotted against each of the input variables in scatter diagrams. Each plot is then subdivided into quadrants whose axes lie on the medians of the input and output variables. The scatter diagrams, subdivided into quadrants, are found in the Appendix to this document. The upper right and lower left quadrants are designated positive, and the other two are designated negative. Then beginning at the rightmost edge of the scatter diagram, points are counted inwards horizontally in the positive quadrant until a point is encountered in the negative quadrant or until the median axis is encountered. Points are counted in a similar manner from the bottom, then from the left, then from the top. The totals for the four quadrants are then summed to give the Olmstead-Tukey⁶ test statistic. If this test statistic exceeds the quantile given in Table II, the output parameter is correlated with the input parameter.

III. THE CURRENT STUDY

For the present study, the TRAC model for the combined injection version of the SCTF with no external steam source and no blockages was run until the lower plenum reached its minimum liquid inventory. The input parameters to be varied were selected and the initializing program was executed to give the set of inputs for the calculations. These eleven input parameters are listed in

TABLE II. QUANTILES FOR THE OLMSTEAD-TUKEY TEST STATISTIC

DECISION RULE. Reject H_0 at the level of significance α if T_4 exceeds the $1 - \alpha$ quantile, $x_{1-\alpha}$, as given below (from Olmstead and Tukey, 1947).

Sample Size	$x_{.80}$	$x_{.90}$	$x_{.95}$	$x_{.99}$	$x_{.999}$
$n = 6$	6	10	—	—	—
$n = 8$	6	8	10	—	—
$n = 10$	6	8	10	14	—
$n = 14$	6	9	10	14	21
$n = \infty$ (use for $n > 14$)	6	8	10	13	18

TABLE III. INPUT VARIABLES FOR THE SCTF SENSITIVITY STUDY

1. Outer iteration convergence criterion (EPSO)
2. Vessel iteration convergence criterion (EPSI)
3. Maximum number of outer iterations (OITMAX)
4. Maximum number of vessel iterations (IITMAX)
5. Maximum temperature change for more conduction nodes for nucleate and transition boiling (DTXHT1)
6. Maximum temperature change for more conduction nodes for other regimes (DTXHT2)
7. Minimum change in axial length below which no more conduction nodes will be inserted (DZNHT)
8. Maximum rows of nodes for the conduction calculation (NZMAX)
9. Minimum time step size (DTMIN)
10. Maximum time step size (DTMAX)
11. Time step accelerator (DDI)

Table III; parentheses enclose the corresponding TRAC variable name. The quantile of the Kendall test statistic for this study was 15, indicating that a minimum of 10 runs was required. In actuality, 11 runs were made.

The calculations each were started from the dump occurring at minimum lower plenum liquid inventory and were run for one CPU hour each. The output parameters that were selected were the amount of reactor time run during the hour, the maximum and minimum time step sizes that actually occurred, and the average time step size. These parameters were then plotted against each of the input variables, and these plots are shown in the appendix to this document.

IV. RESULTS OF THE STUDY

Both the time-step-size accelerator and the maximum allowable time step had a great effect on total reactor time calculated with one hour of CPU time. The tightness of the convergence criteria also affected running time, as would be expected. One should note that these input variable changes did not alter the quantitative results of the calculation; they altered only the amount of

time required to run the problem. This result increases our confidence in the TRAC code results.

The most efficient combination of these input variables, therefore, has been extrapolated from the results of this study and is shown in Table IV. The increase in efficiency should save on the order of three hours execution time for each calculation, which is a significant savings in view of the total number of calculations scheduled for FY 1981.

V. ACKNOWLEDGMENTS

Without the initializing program written by P. J. Hodson and the plotting program written by M. W. Cappiello, this study would have been much more difficult than it was. Without the help and encouragement of R. D. Burns III, it would have been impossible.

TABLE IV. EXTRAPOLATED OPTIMAL COMBINATION OF INPUT VARIABLES

1.	EPSO	0.005
2.	EPSI	0.00001
3.	OITMAX	50
4.	IITMAX	75-90
5.	DTXHT1	4 K
6.	DTXHT2	10 K
7.	DZNHT	0.04 m
8.	NZMAX	100
9.	DTMIN	0.00008
10.	DTMAX	0.0001
11.	DDI	1.01

REFERENCES

1. "TRAC-PD2: An Advanced Best-Estimate Computer Program for Pressurized Water Reactor Loss-of-Coolant Accident Analysis," Los Alamos National Laboratory report (to be published).
2. S. T. Smith, "Comparison of the TRAC Computational Results for the Slab Core Test Facility Model and the Reference German PWR During Reflood," Los Alamos National Laboratory report LA-8704-MS (in press).
3. R. D. Burns III, "Method for Statistical Analysis Based on a Small Number of Observations," in Nuclear Reactor Safety Quarterly Progress Report, April 1-June 30, 1978, J. F. Jackson and M. G. Stevenson, Comp., Los Alamos National Laboratory Report LA-7481-PR, NUREG/CR-0385 (October 1978).
4. M. G. Kendall, Rank Correlation Methods, 2nd ed., (Hafner, New York, 1955).
5. W. J. Conover, Practical Nonparametric Statistics, (John Wiley Sons Inc., New York, 1971).
6. P. S. Olmstead and J. W. Tukey, "A Corner Test for Association," Ann Math Stat, 18, 495-513 (1947).

APPENDIX

SCATTER DIAGRAMS OF THE SELECTED OUTPUT PARAMETERS AS A FUNCTION OF THE INPUT VARIABLES

This appendix contains plots of all the discrete values of the selected output parameters for each of the eleven calculations as functions of the discrete values of the input variables. From these plots, following the method outlined in Section II, the results given in Table IV can be verified easily.

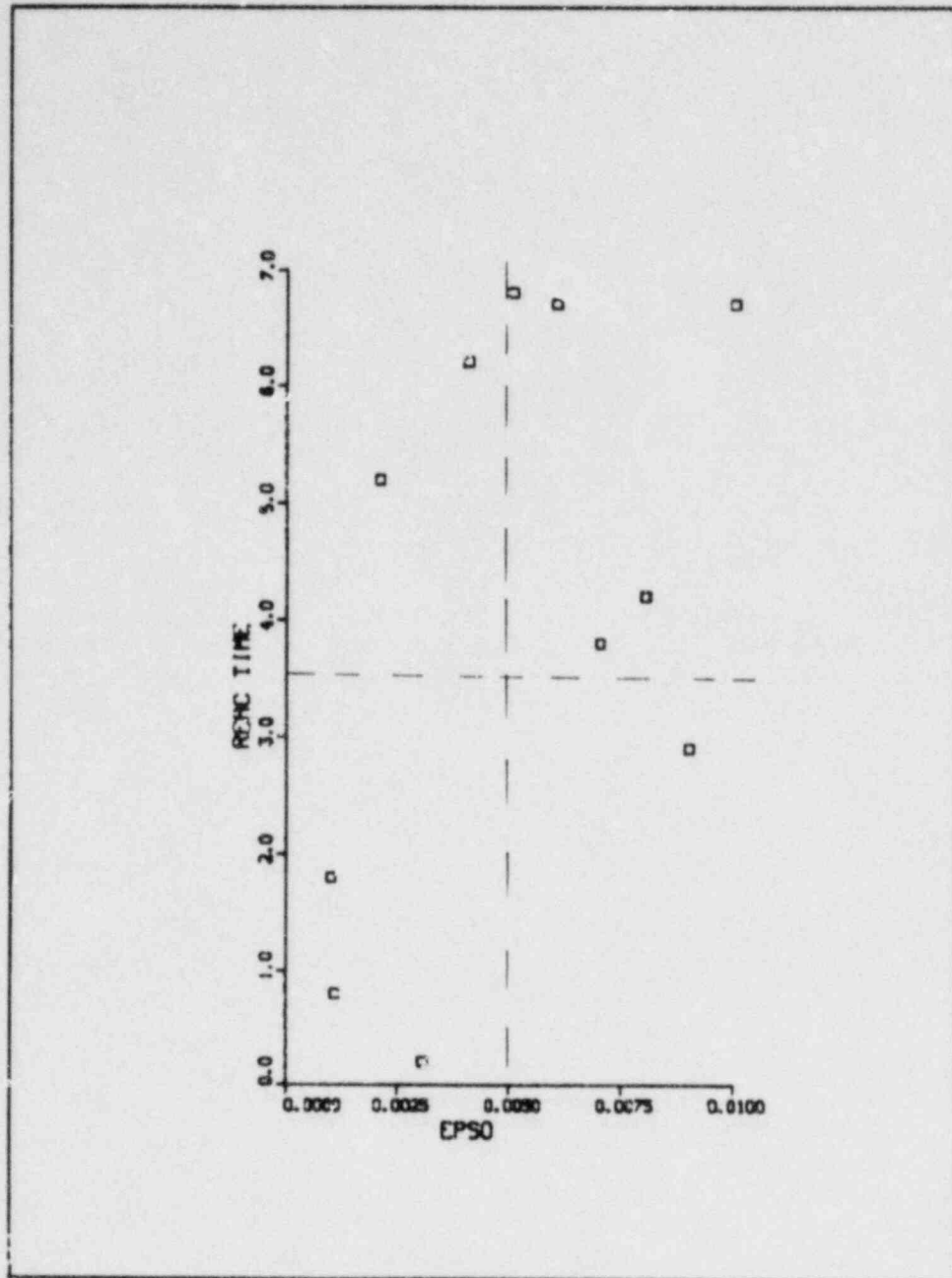


Fig. 1. Reactor time as a function of outer iteration convergence criterion.

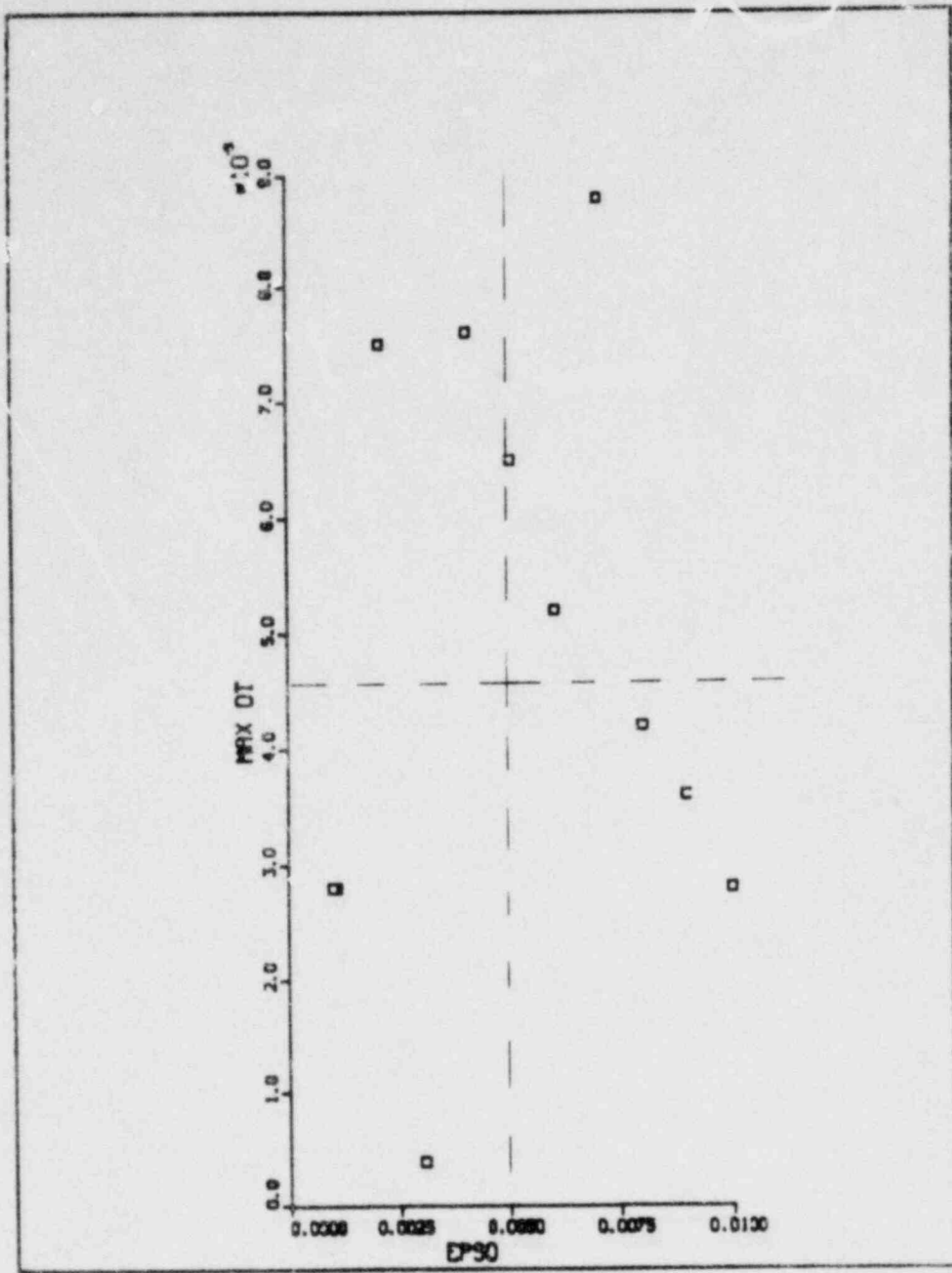


Fig. 2. Maximum time step size as a function of outer iteration convergence criterion.

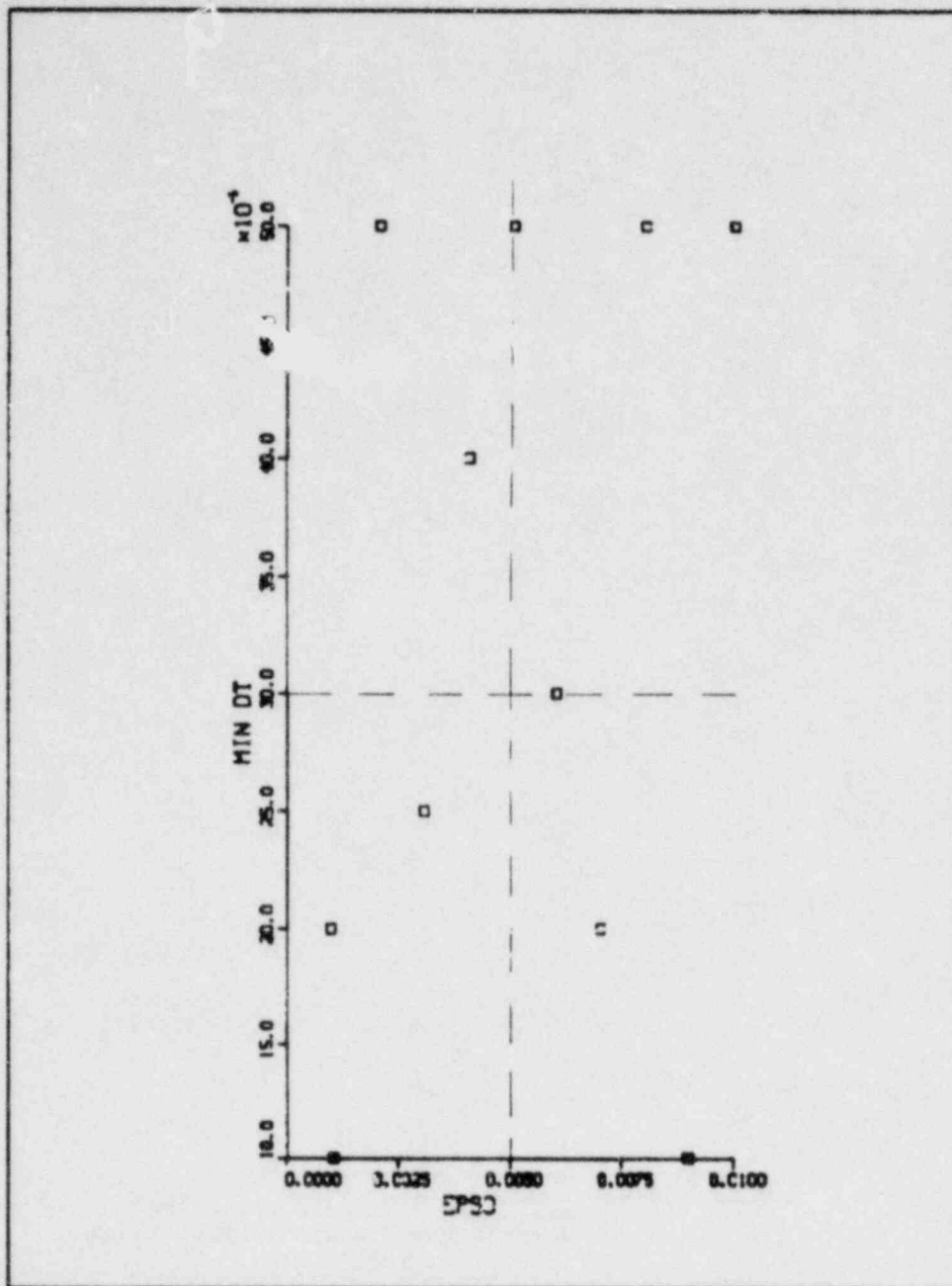


Fig. 3. Minimum time step size as a function of outer iteration convergence criterion.

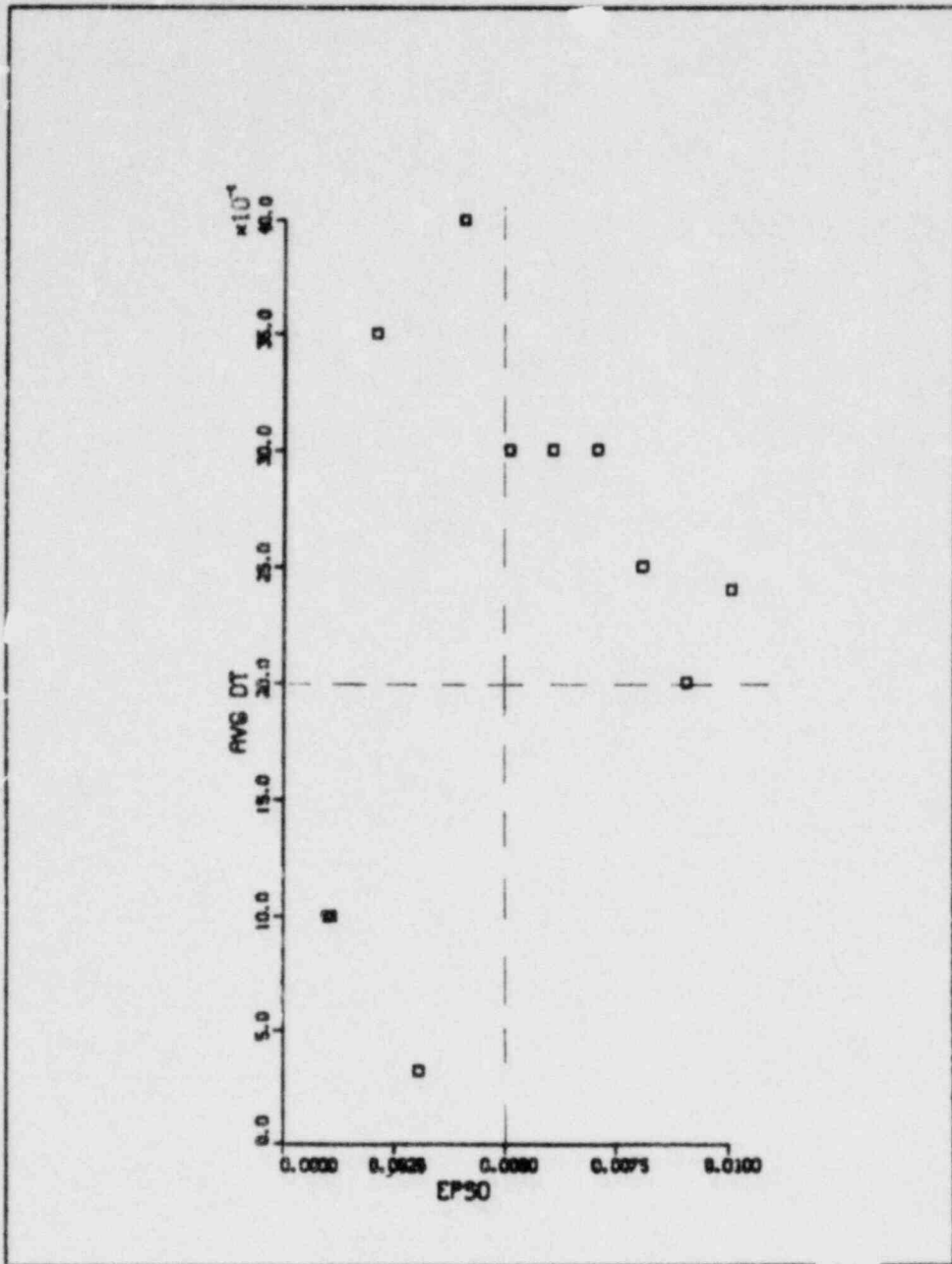


Fig. 4. Average time step size as a function of outer iteration convergence criterion.

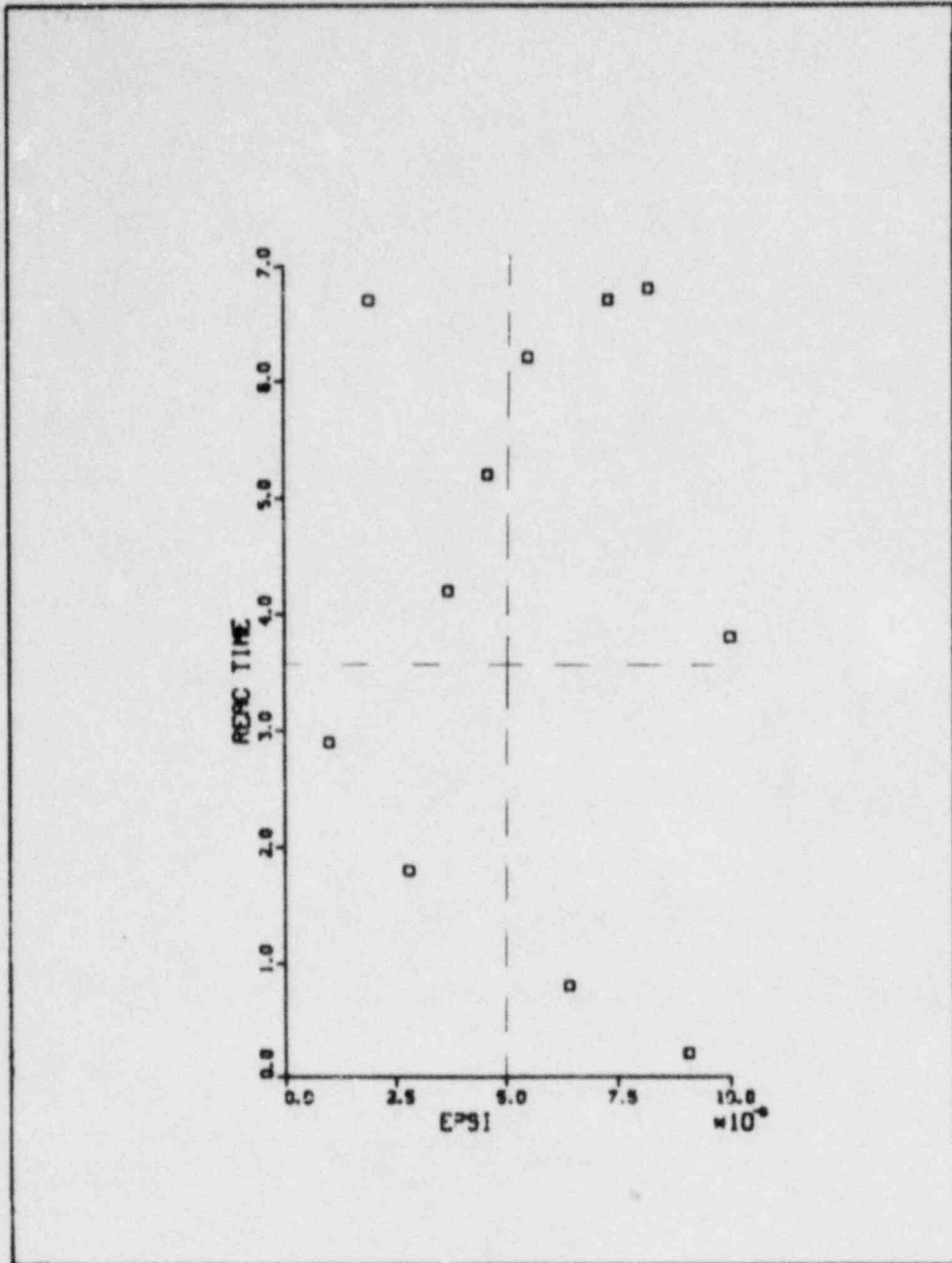


Fig. 5. Reactor time as a function of inner iteration convergence criterion.

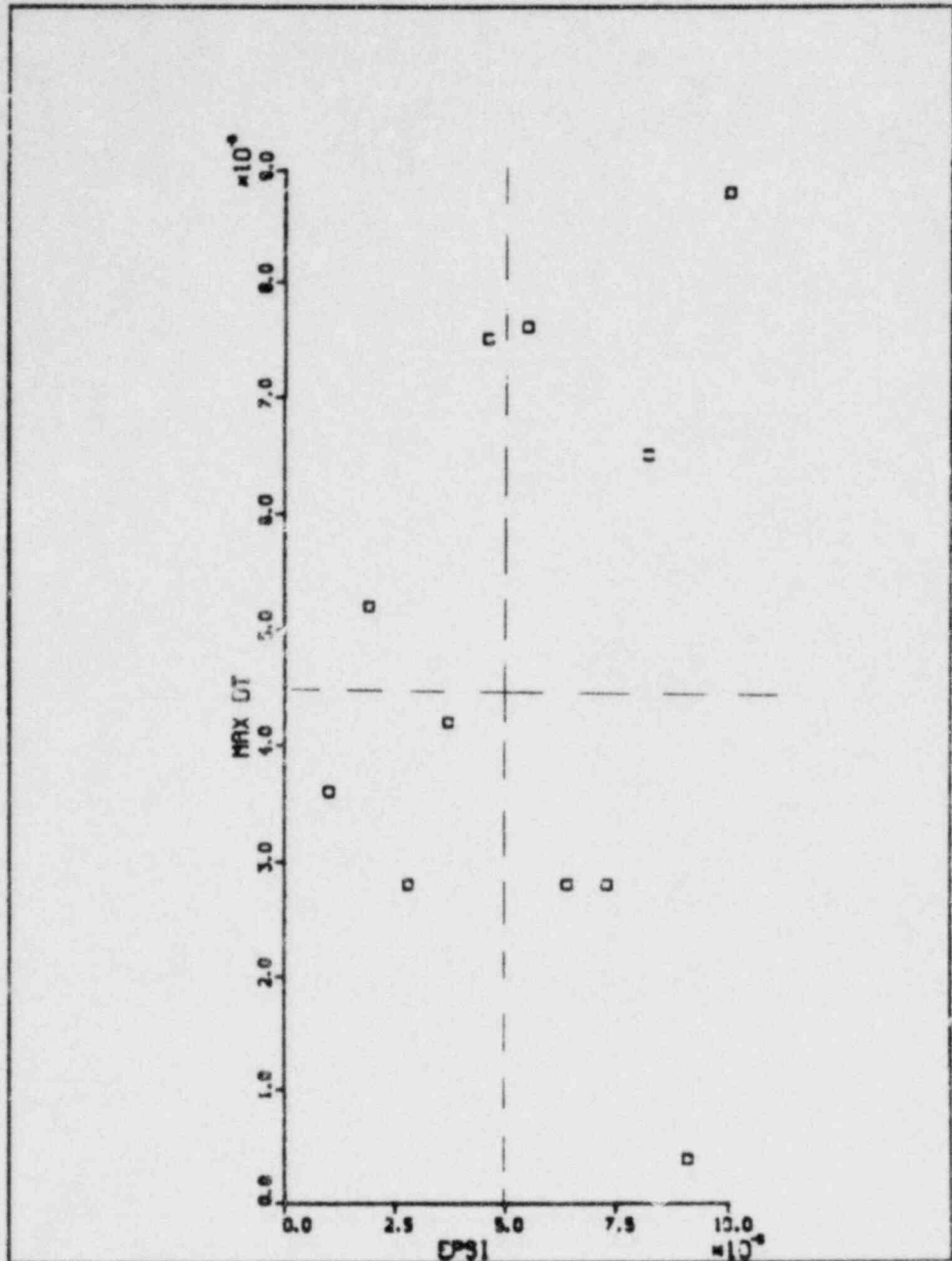


Fig. 6. Maximum time step size as a function of inner iteration convergence criterion.

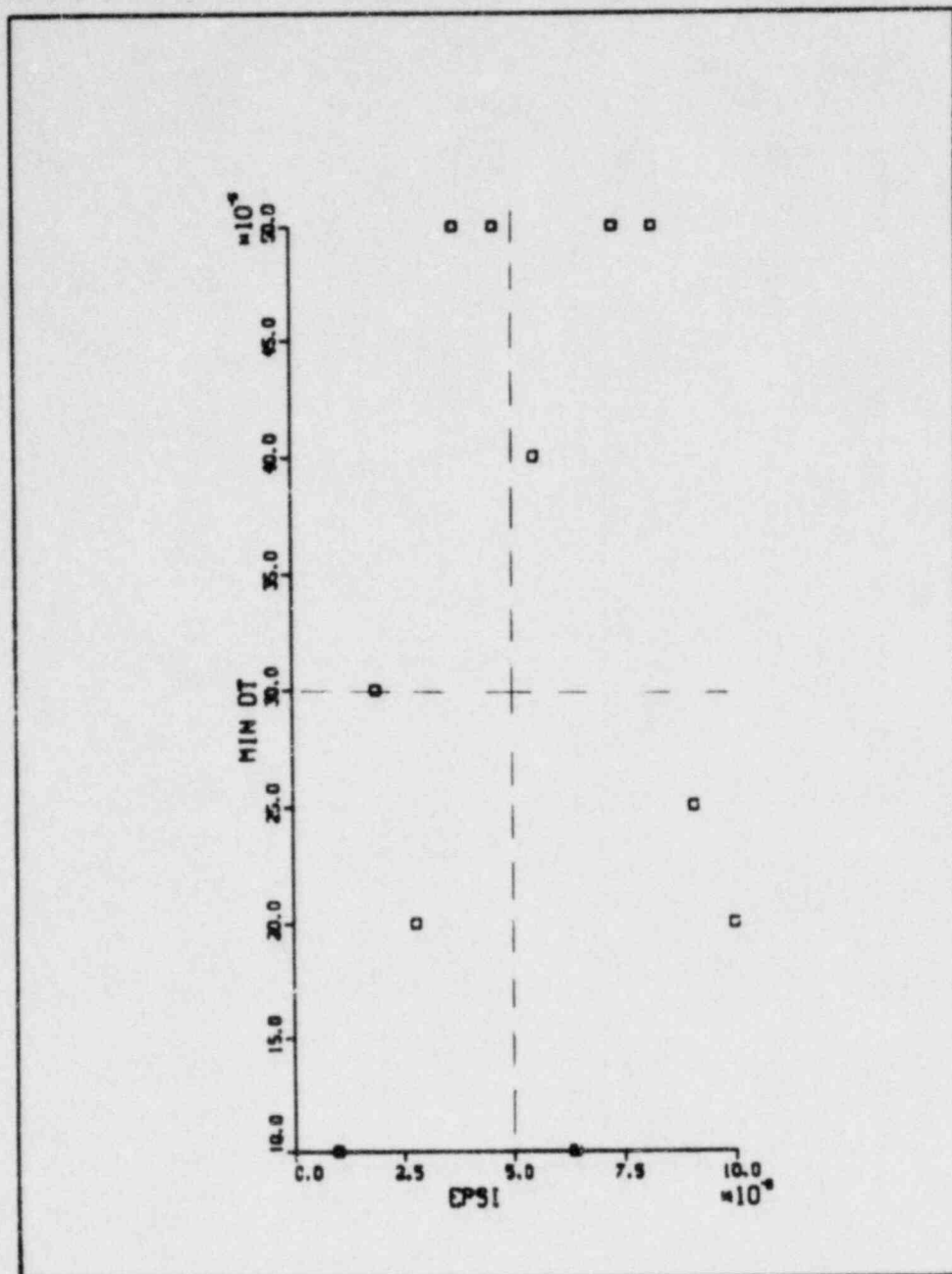


Fig. 7. Minimum time step size as a function of inner iteration convergence criterion.

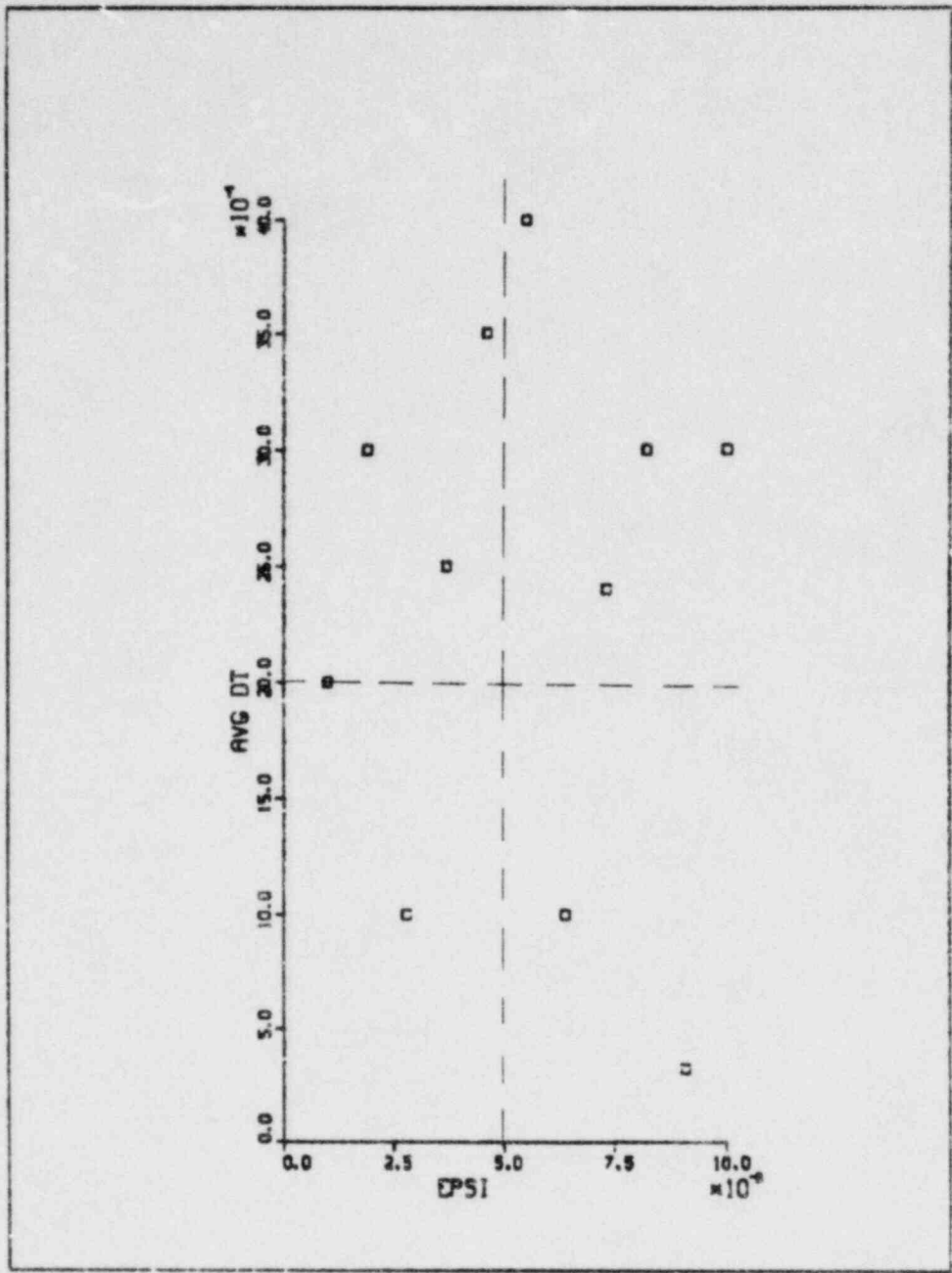


Fig. 8. Average time step size as a function of inner iteration convergence criterion.

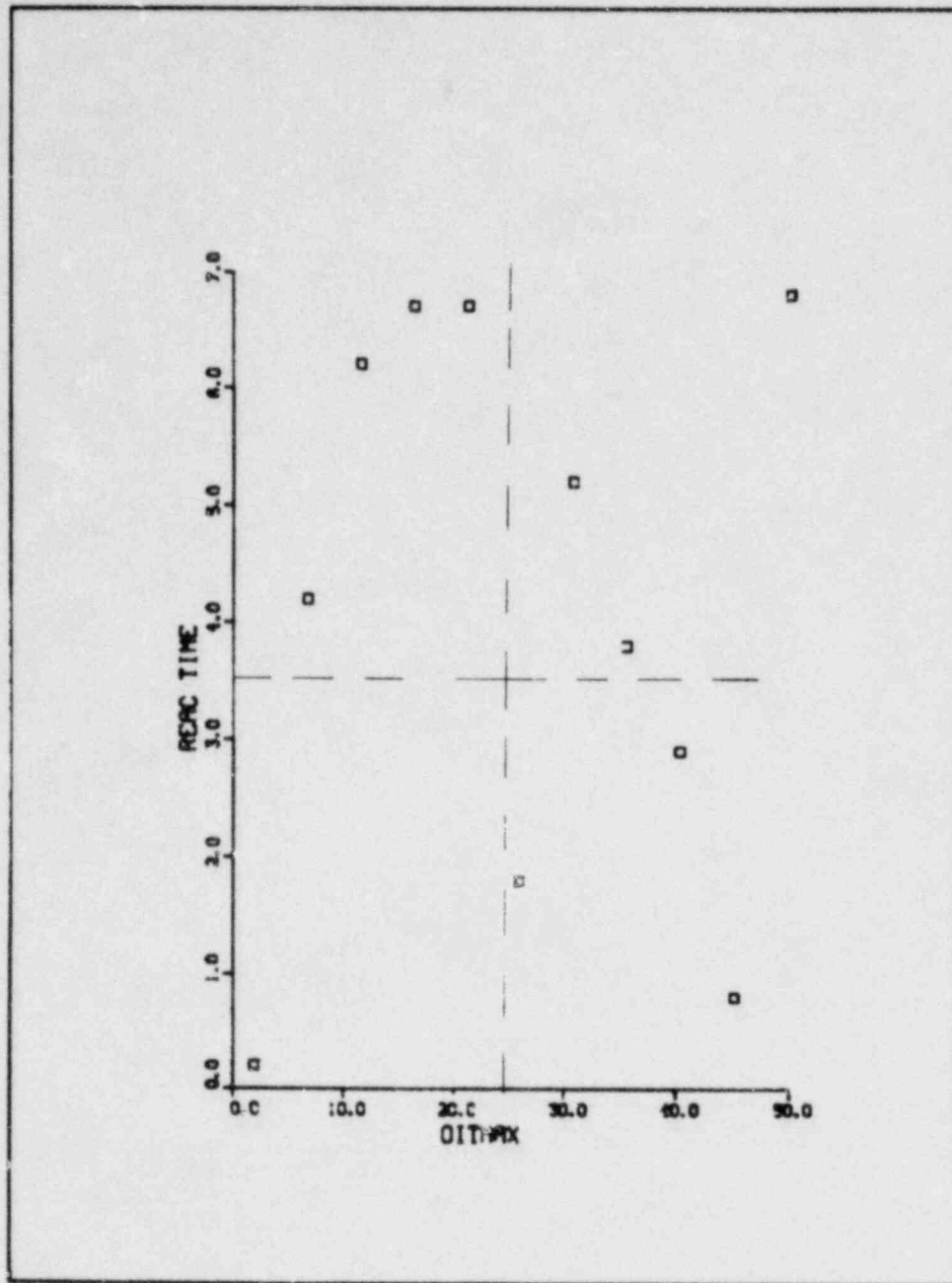


Fig. 9. Reactor time as a function of maximum number of outer iterations.

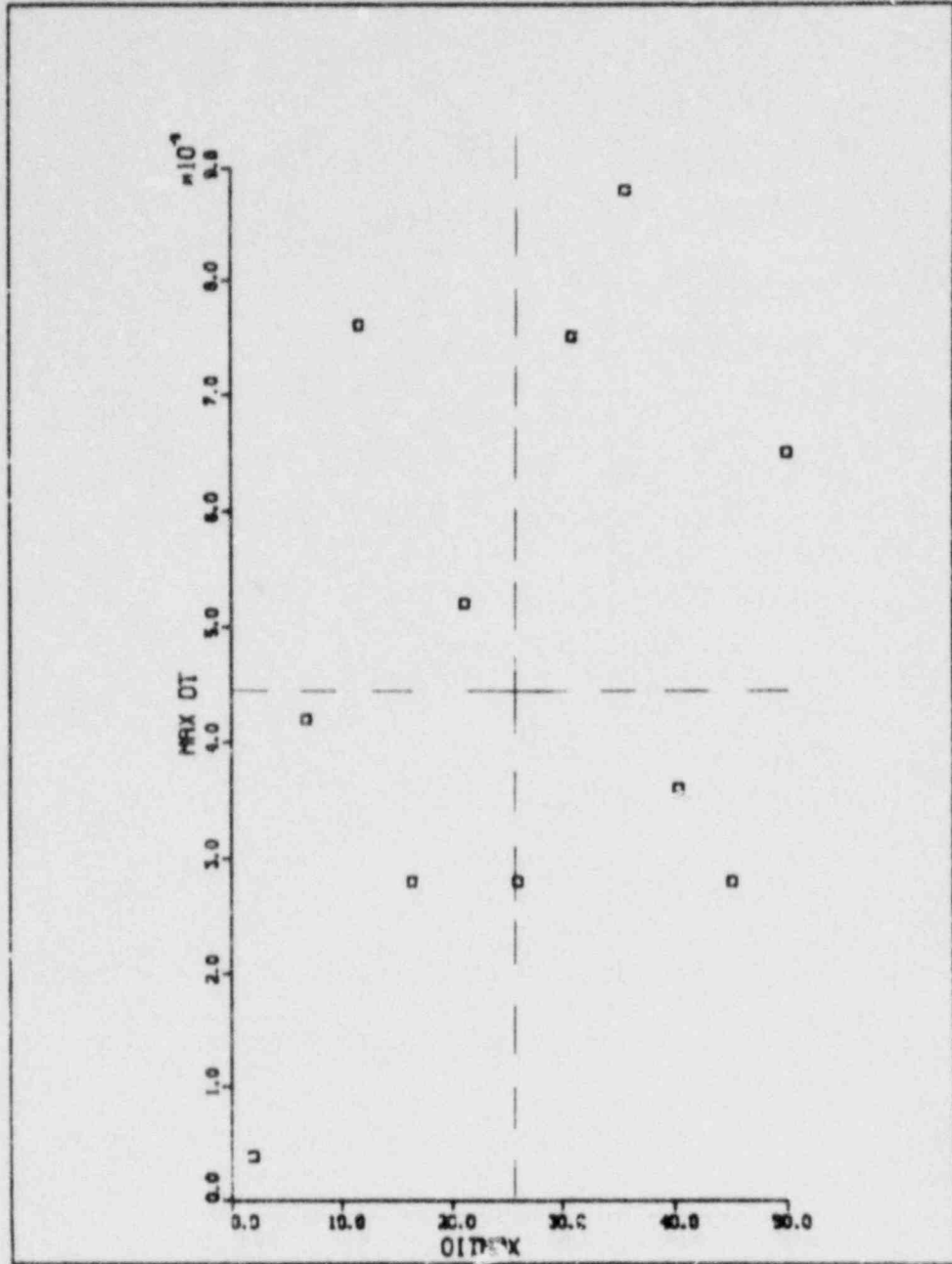


Fig. 10. Maximum time step size as a function of maximum number of outer iterations.

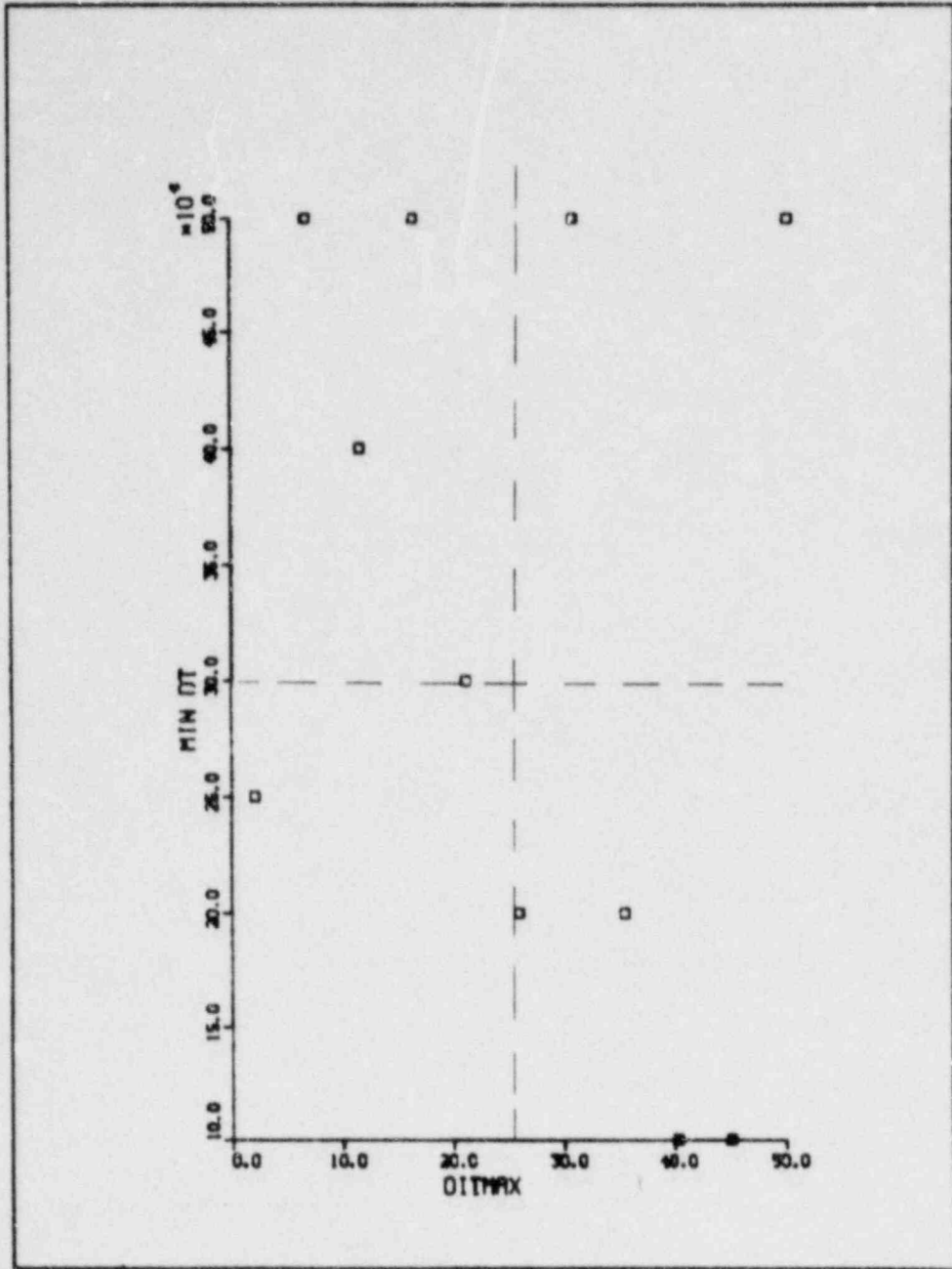


Fig. 11. Minimum time step size as a function of maximum number of outer iterations.

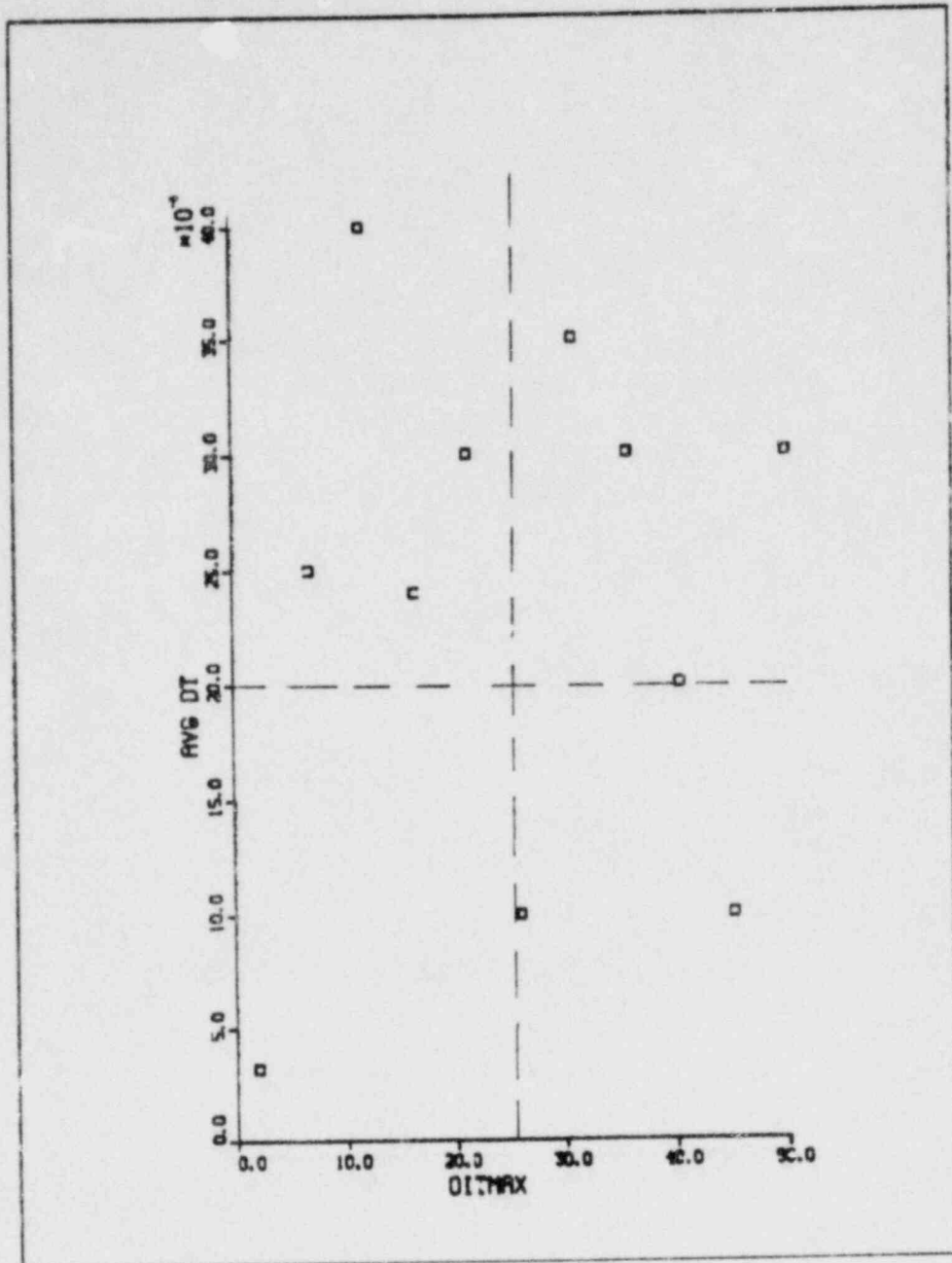


Fig. 12. Average time step size as a function of maximum number of outer iterations.

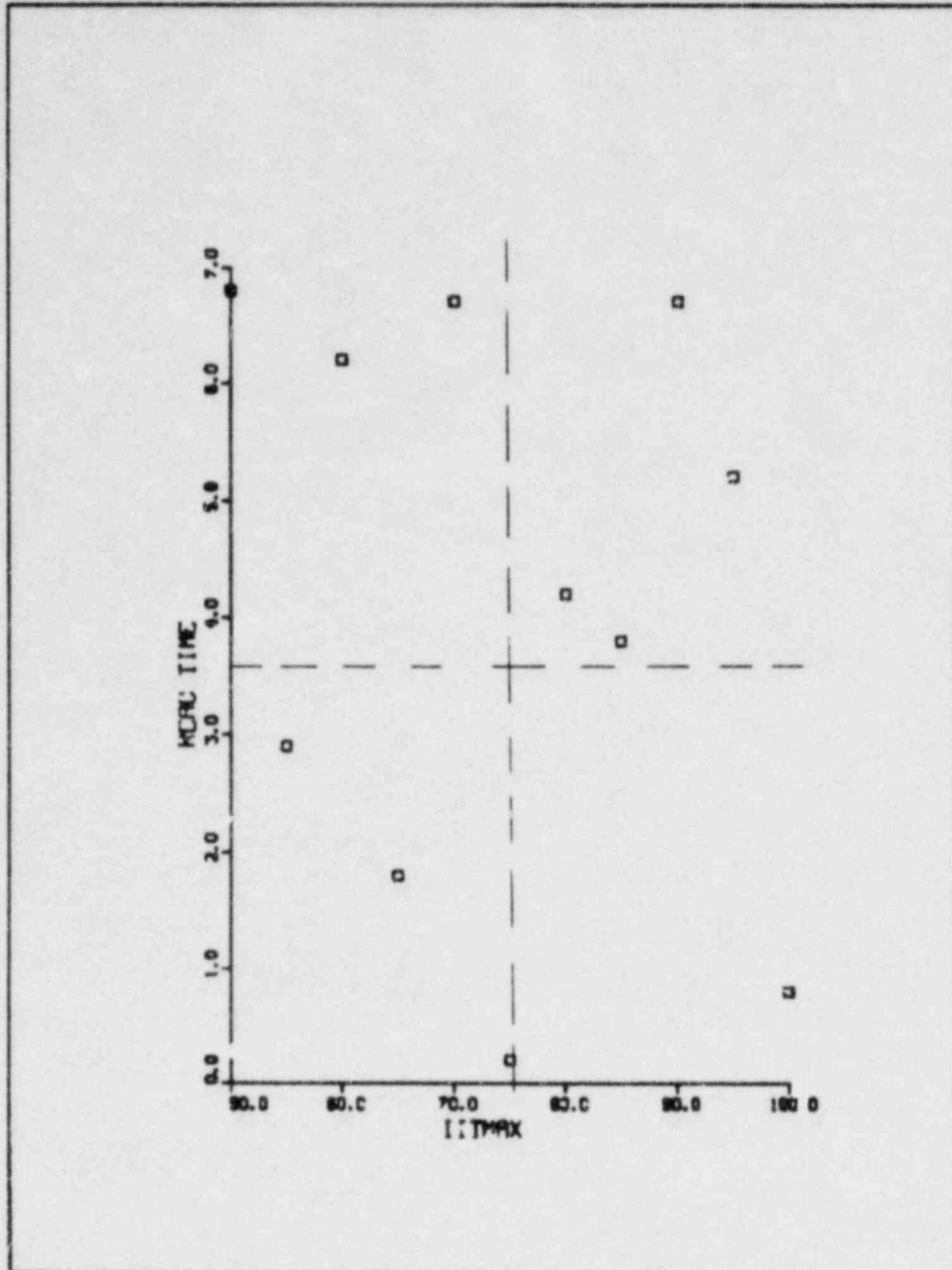


Fig. 13. Reactor time as a function of maximum number of vessel iterations.

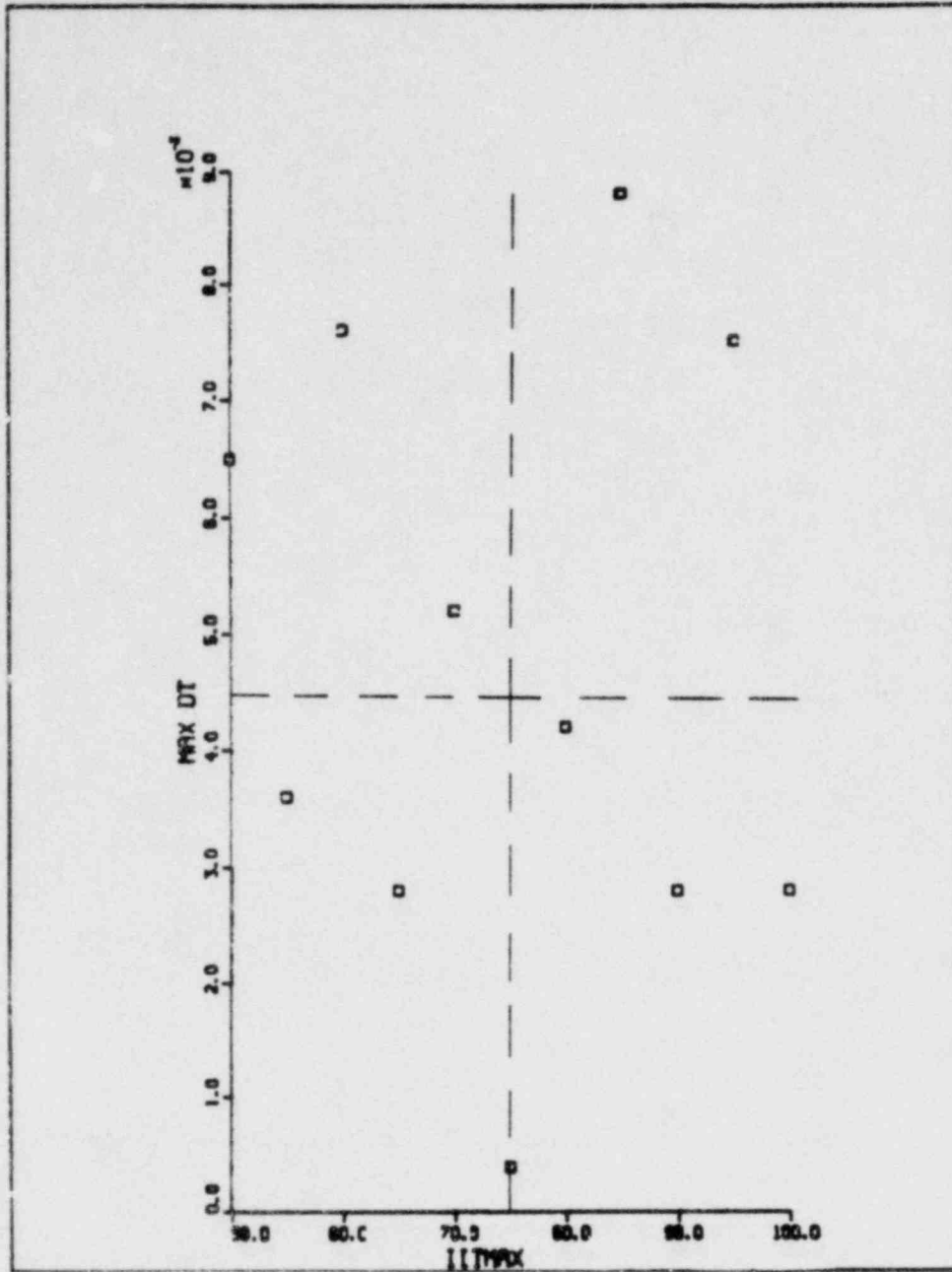


Fig. 14. Maximum time step size as a function of maximum number of vessel iterations.

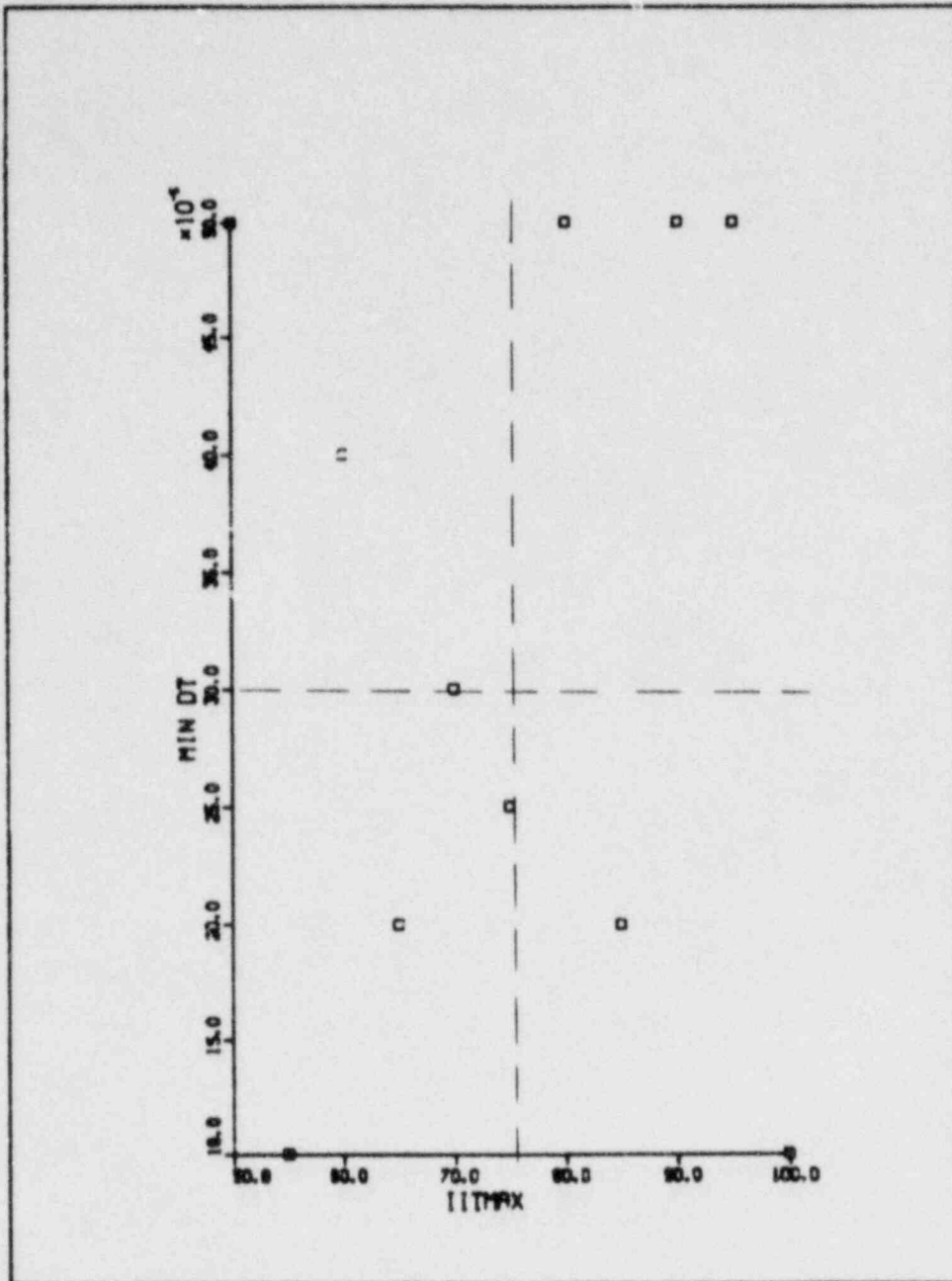


Fig. 15. Minimum time step size as a function of maximum number of vessel iterations.

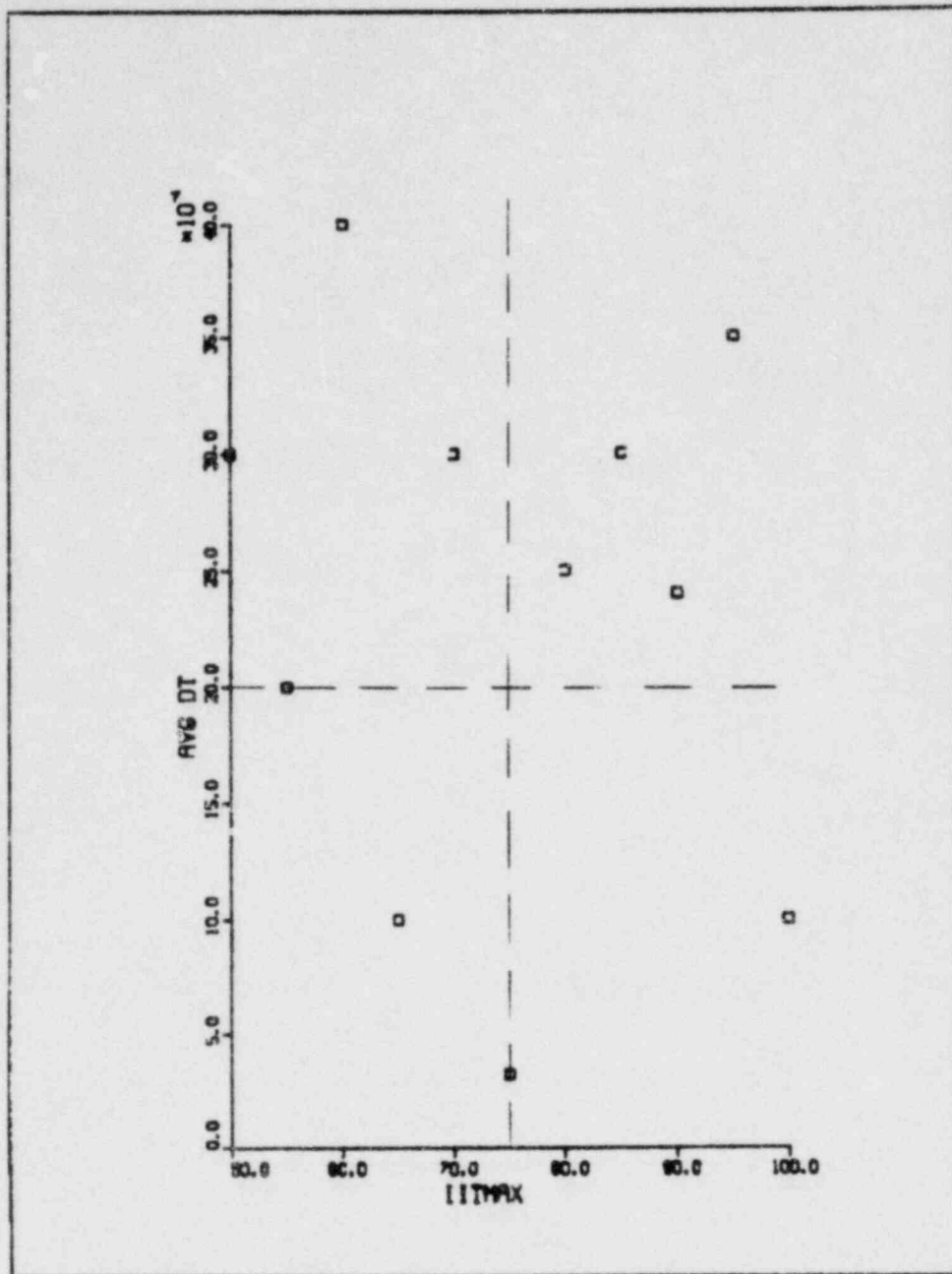


Fig. 16. Average time step size as a function of maximum number of vessel iterations.

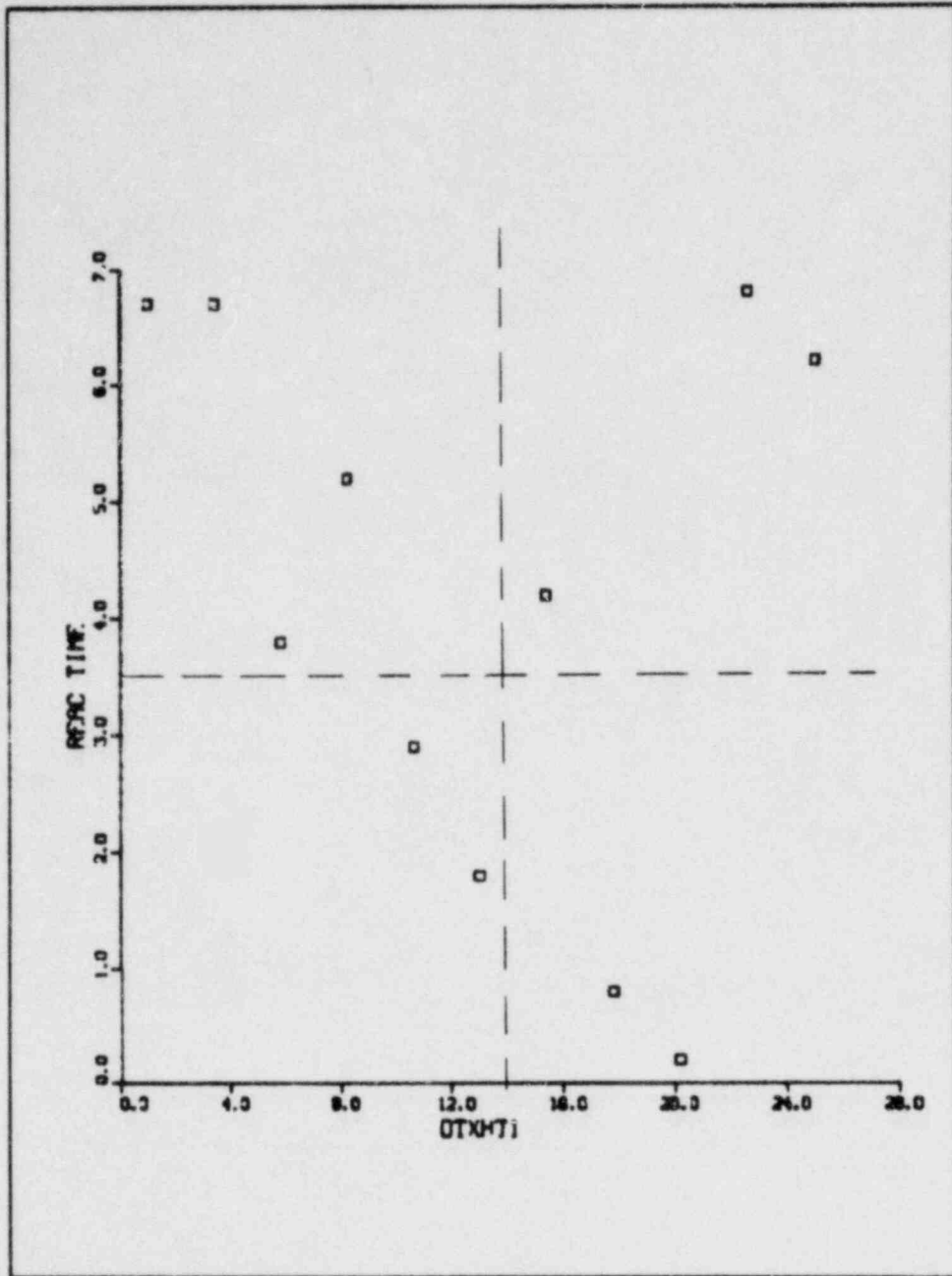


Fig. 17. Reactor time as a function of maximum temperature change for more conduction nodes for nucleate and transition boiling.

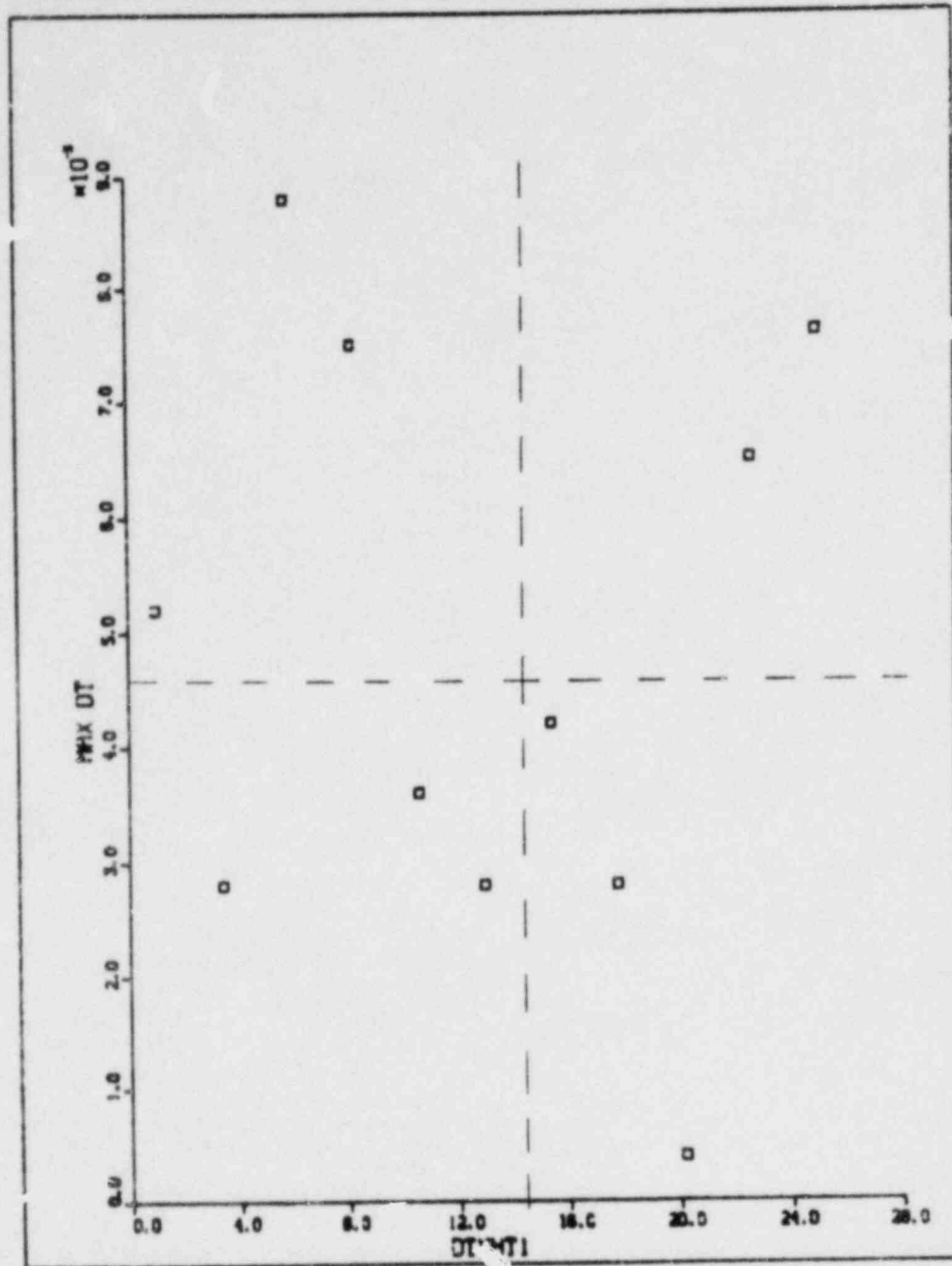


Fig. 18. Maximum time step size as a function of maximum temperature change for more conduction nodes for nucleate and transition boiling.

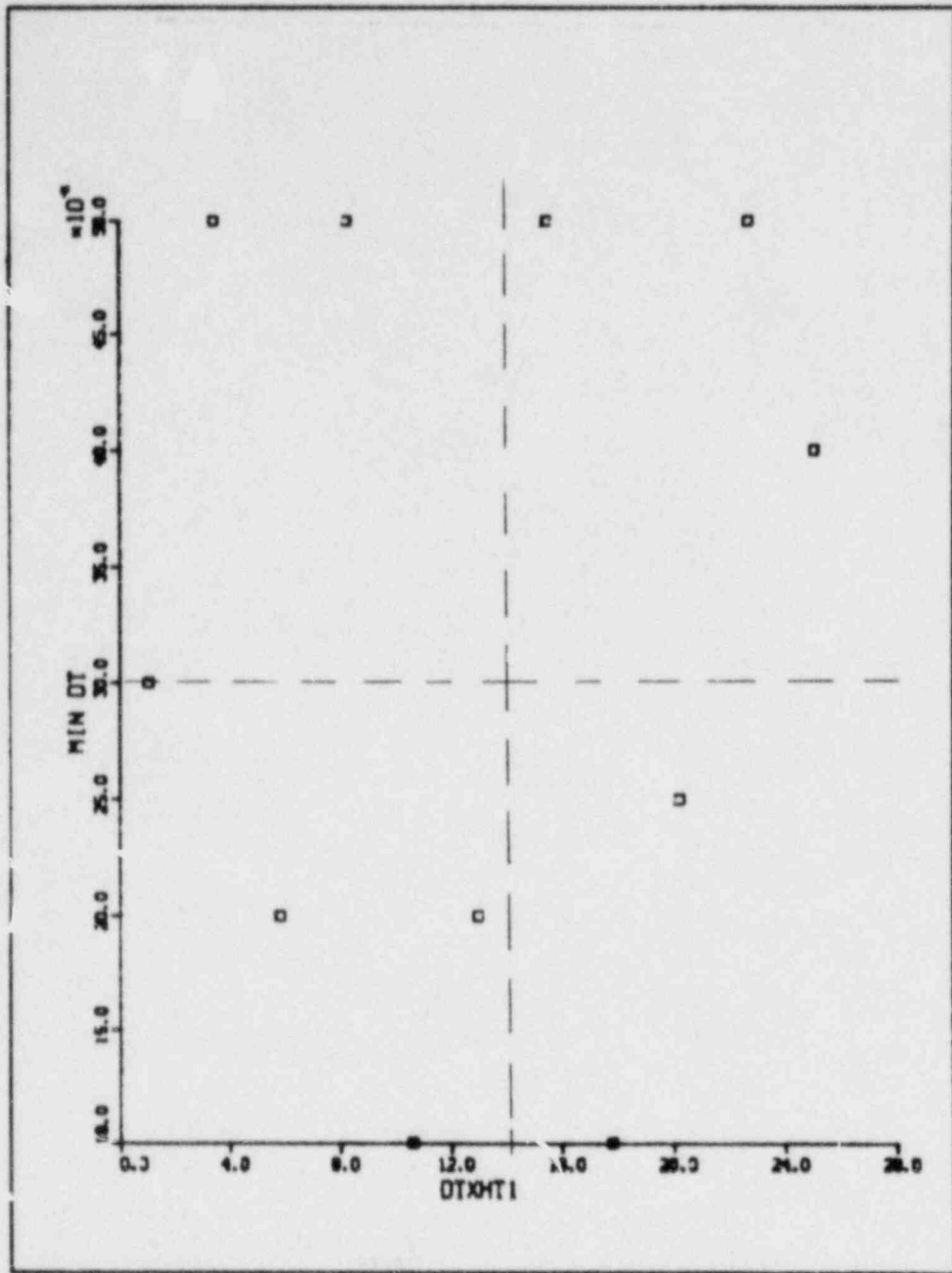


Fig. 19. Minimum time step size as a function of maximum temperature change for more conduction nodes for nucleate and transition boiling.

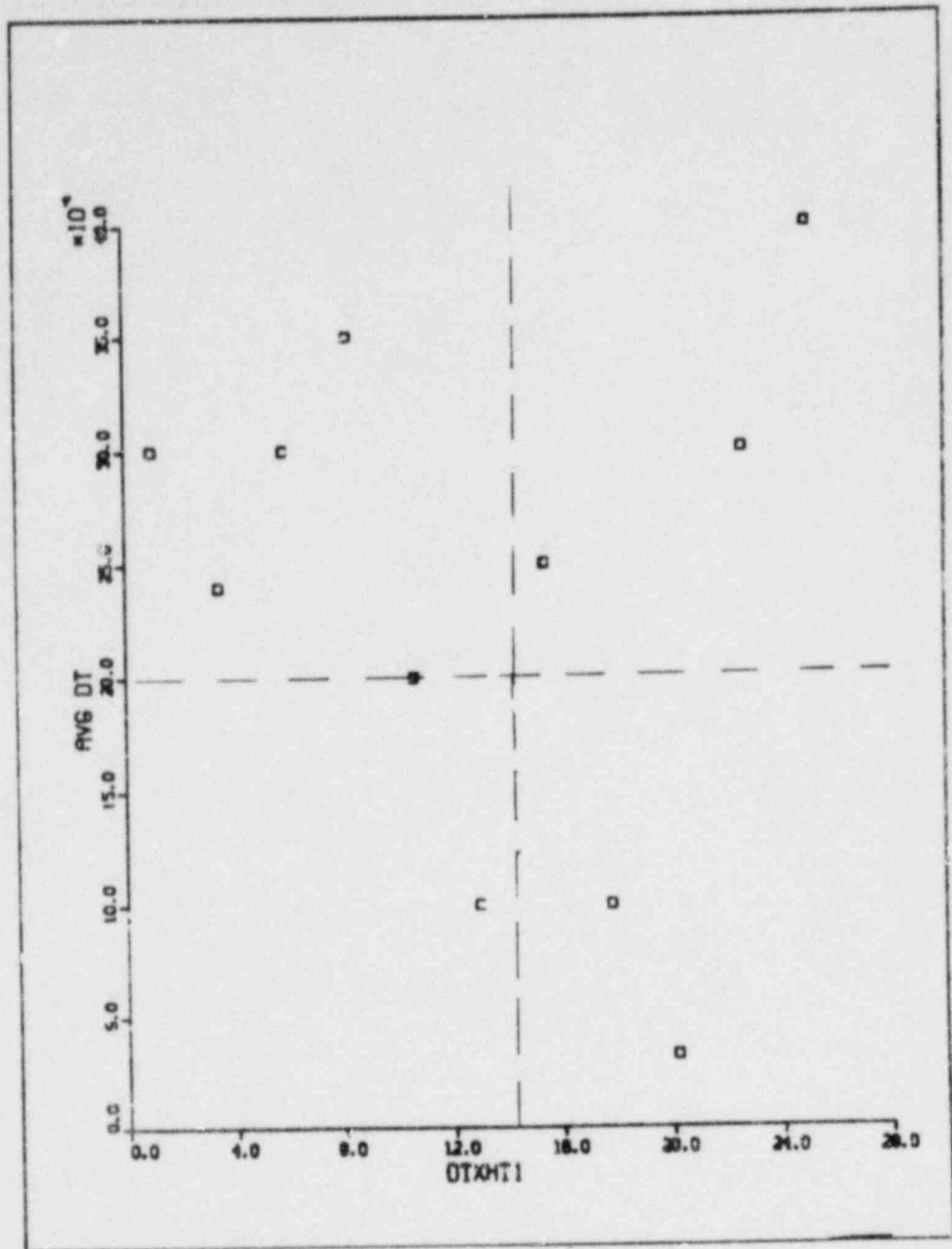


Fig. 20. Average time step size as a function of maximum temperature change for more conduction nodes for nucleate and transition boiling.

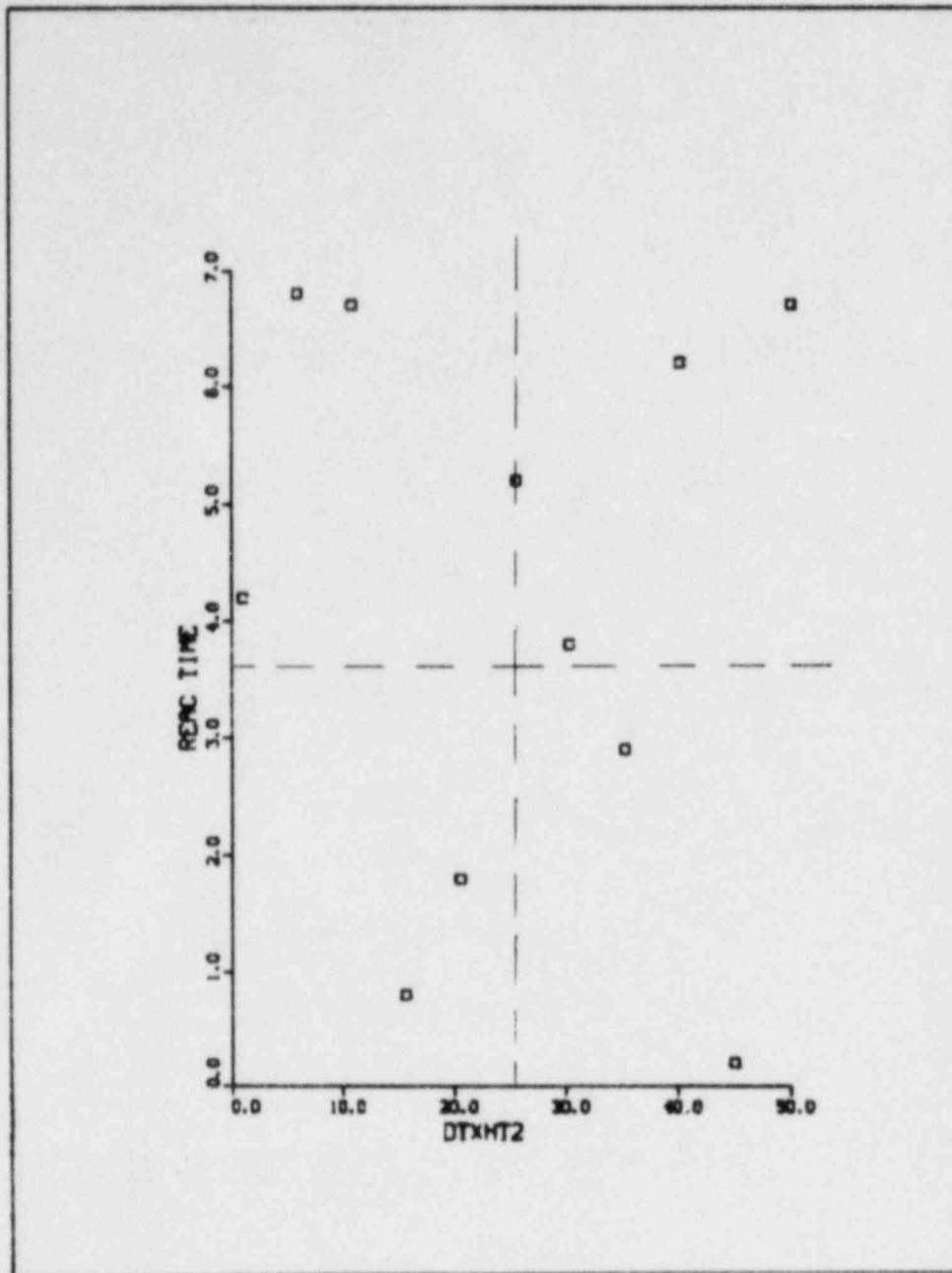


Fig. 21. Reactor time as a function of maximum temperature change for more conduction nodes for other regimes.

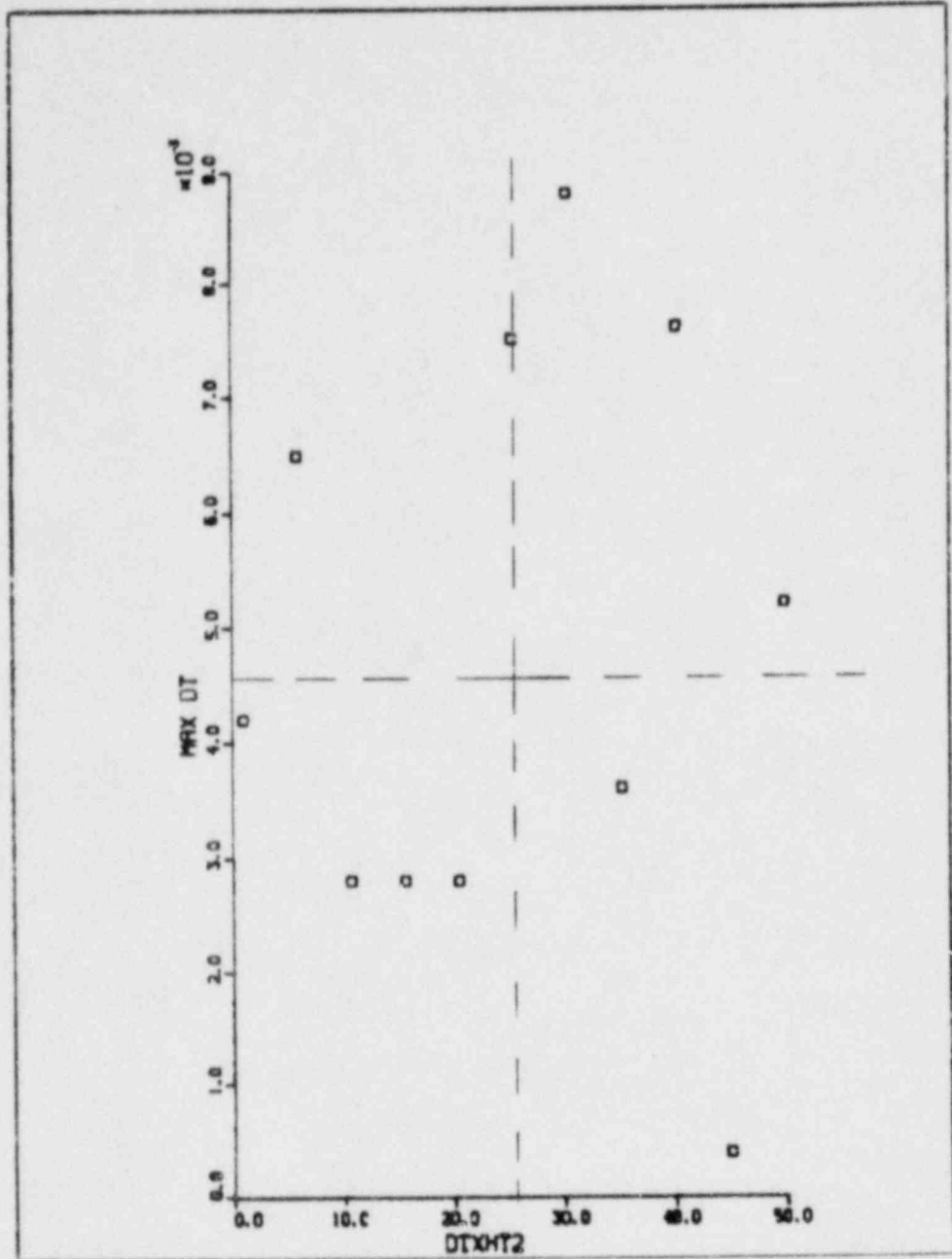


Fig. 22. Maximum time step size as a function of maximum temperature change for more conduction nodes for other regimes.

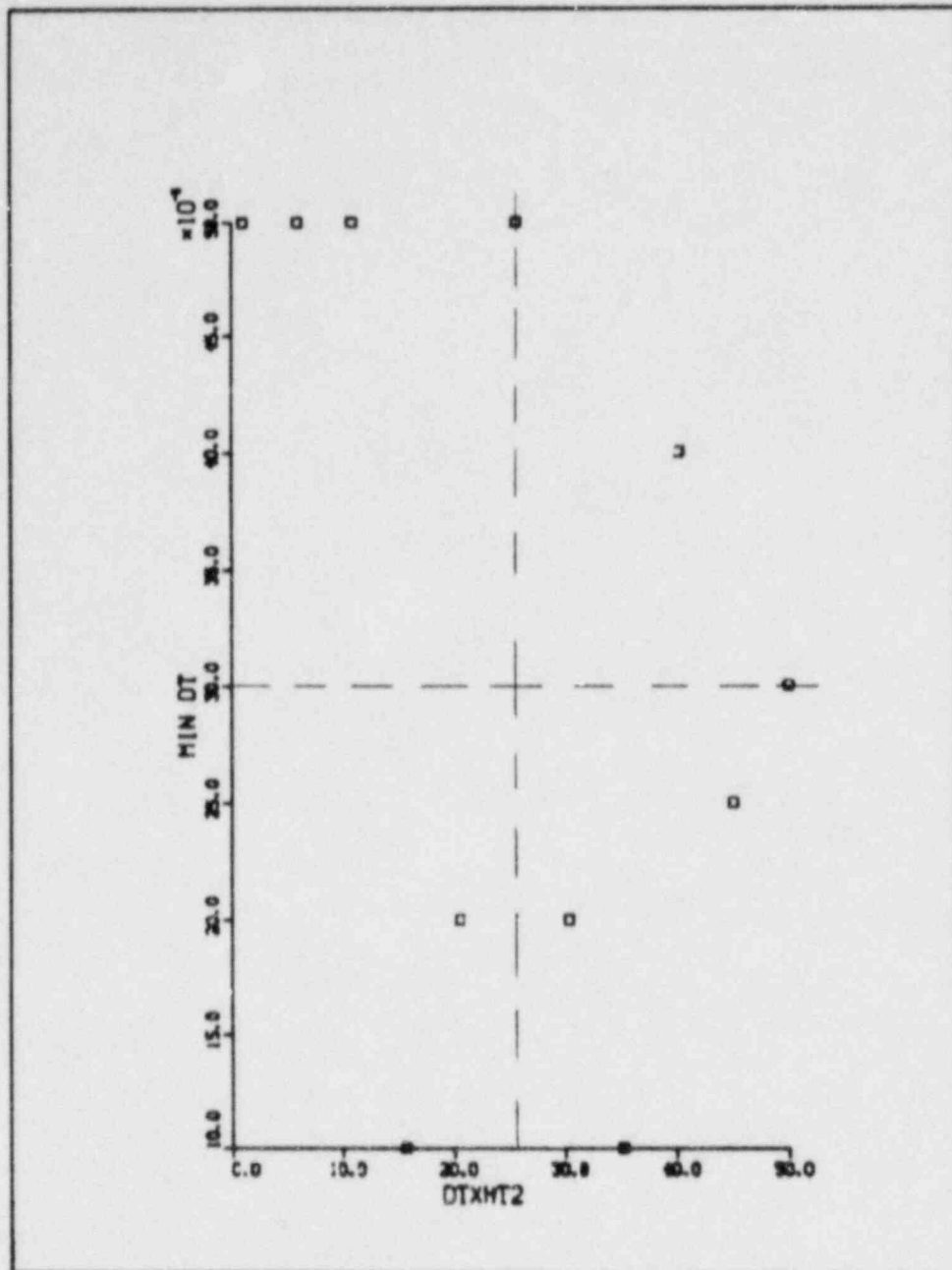


Fig. 23. Minimum time step size as a function of maximum temperature change for more conduction nodes for other regimes.

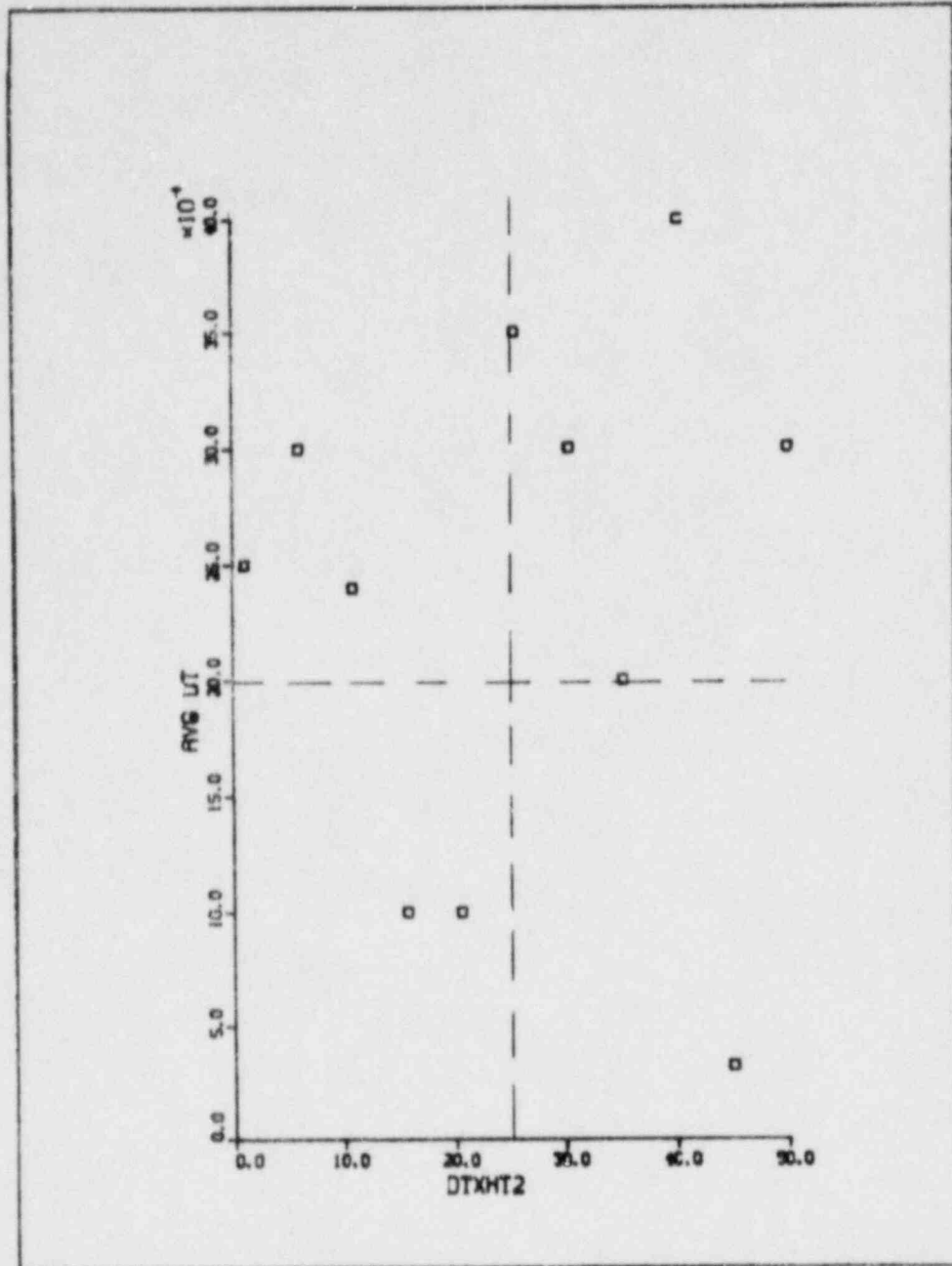


Fig. 24. Average time step size as a function of maximum temperature change for more conduction nodes for other regimes.

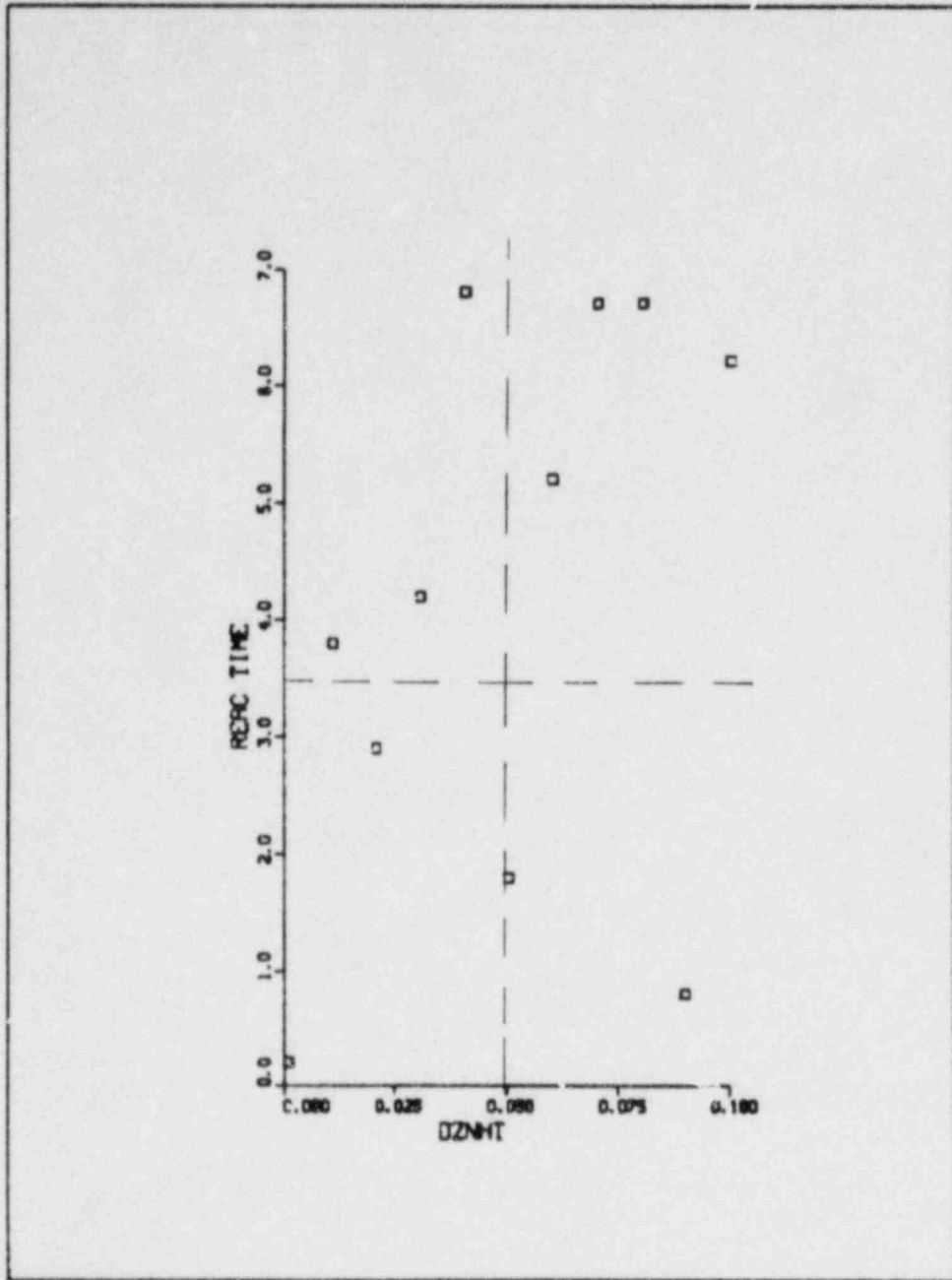


Fig. 25. Reactor time as a function of minimum change below which no more conduction nodes will be inserted.

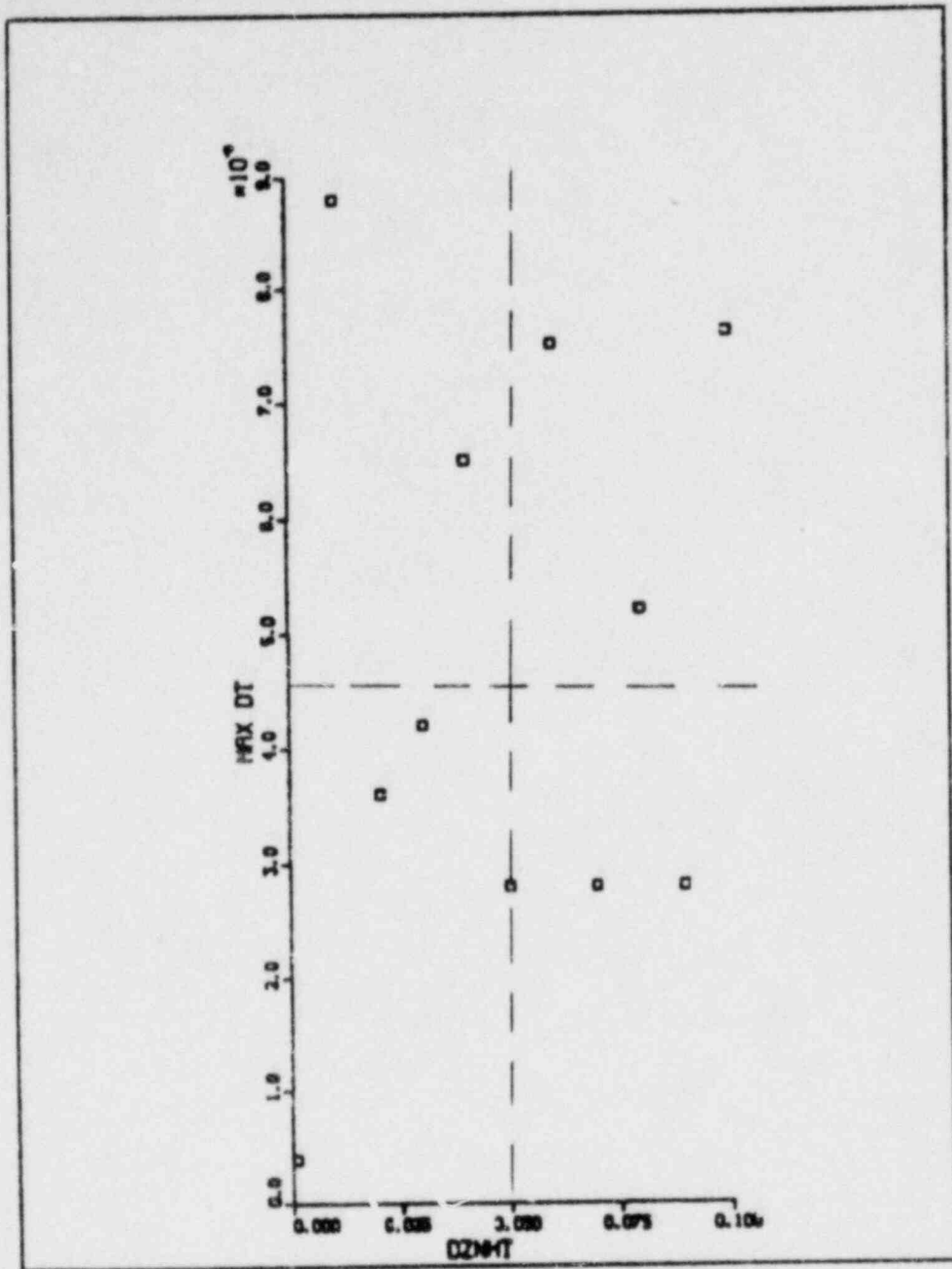


Fig. 26. Maximum time step size as a function of minimum change below which no more conduction nodes will be inserted.

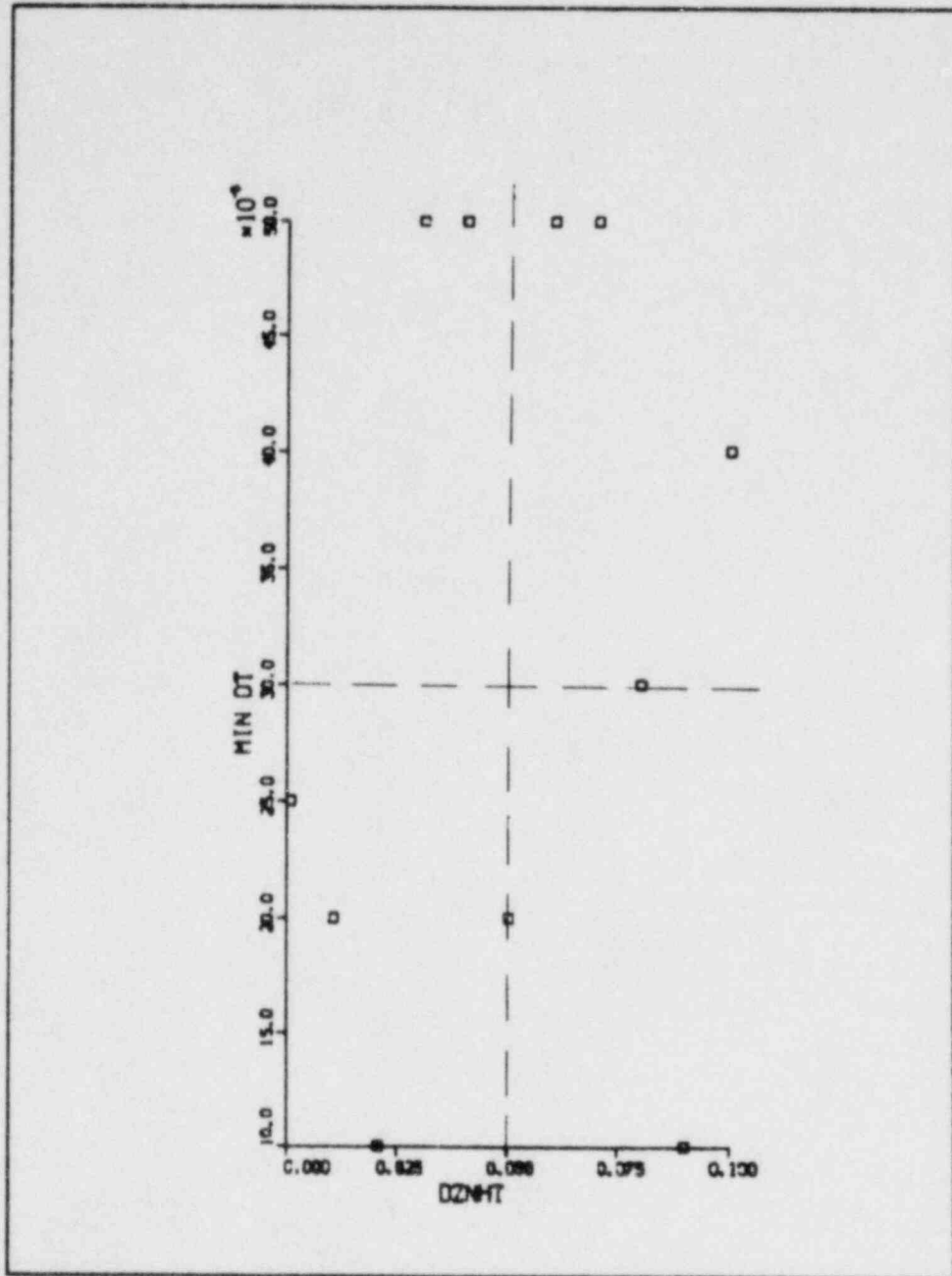


Fig. 27. Minimum time step size as a function of minimum change below which no more conduction nodes will be inserted.

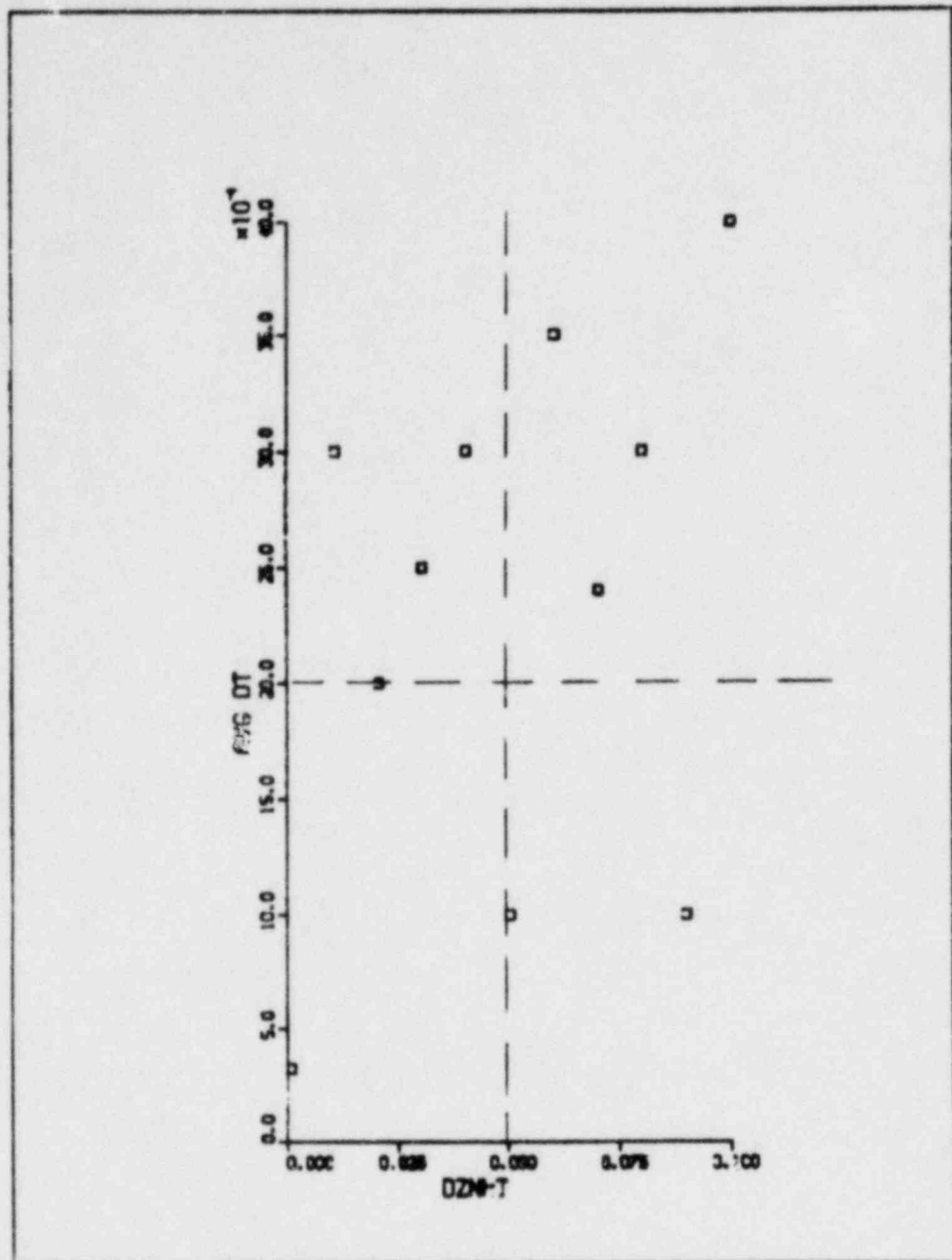


Fig. 28. Average time step size as a function of minimum change below which no more conduction nodes will be inserted.

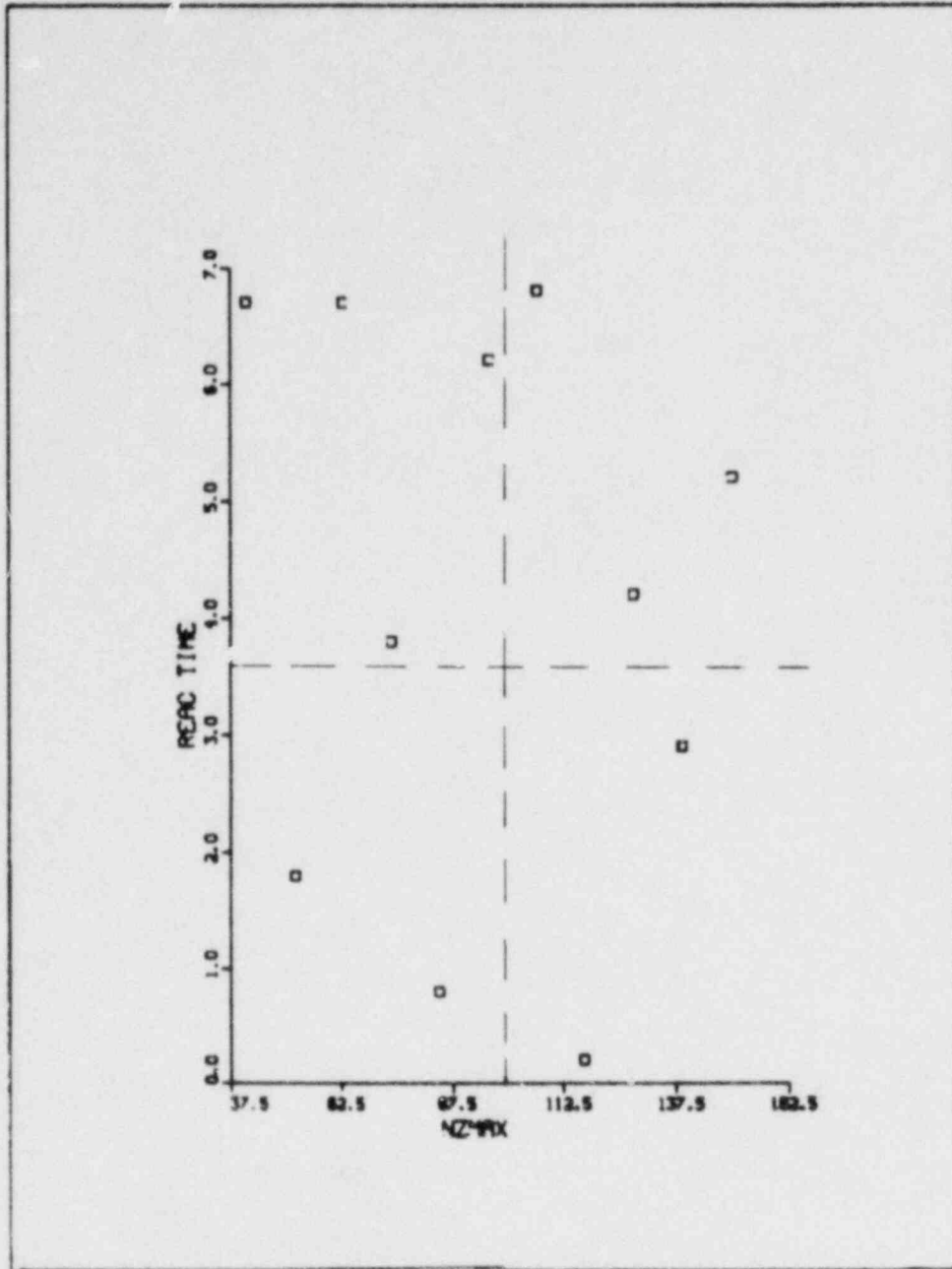


Fig. 29. Reactor time as a function of maximum rows of nodes for the conduction calculation.

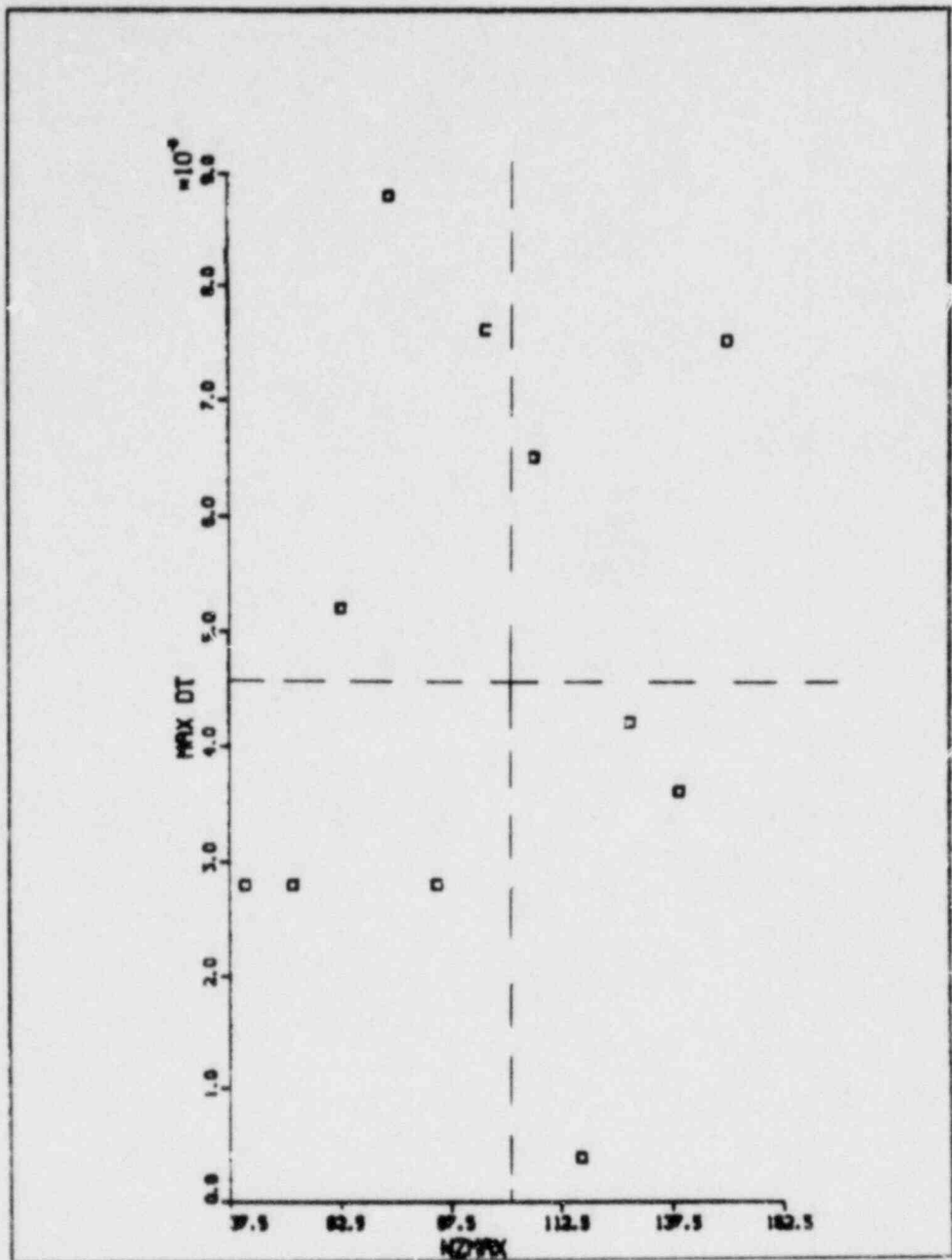


Fig. 30. Maximum time step size as a function of maximum rows of nodes for the conduction calculation.

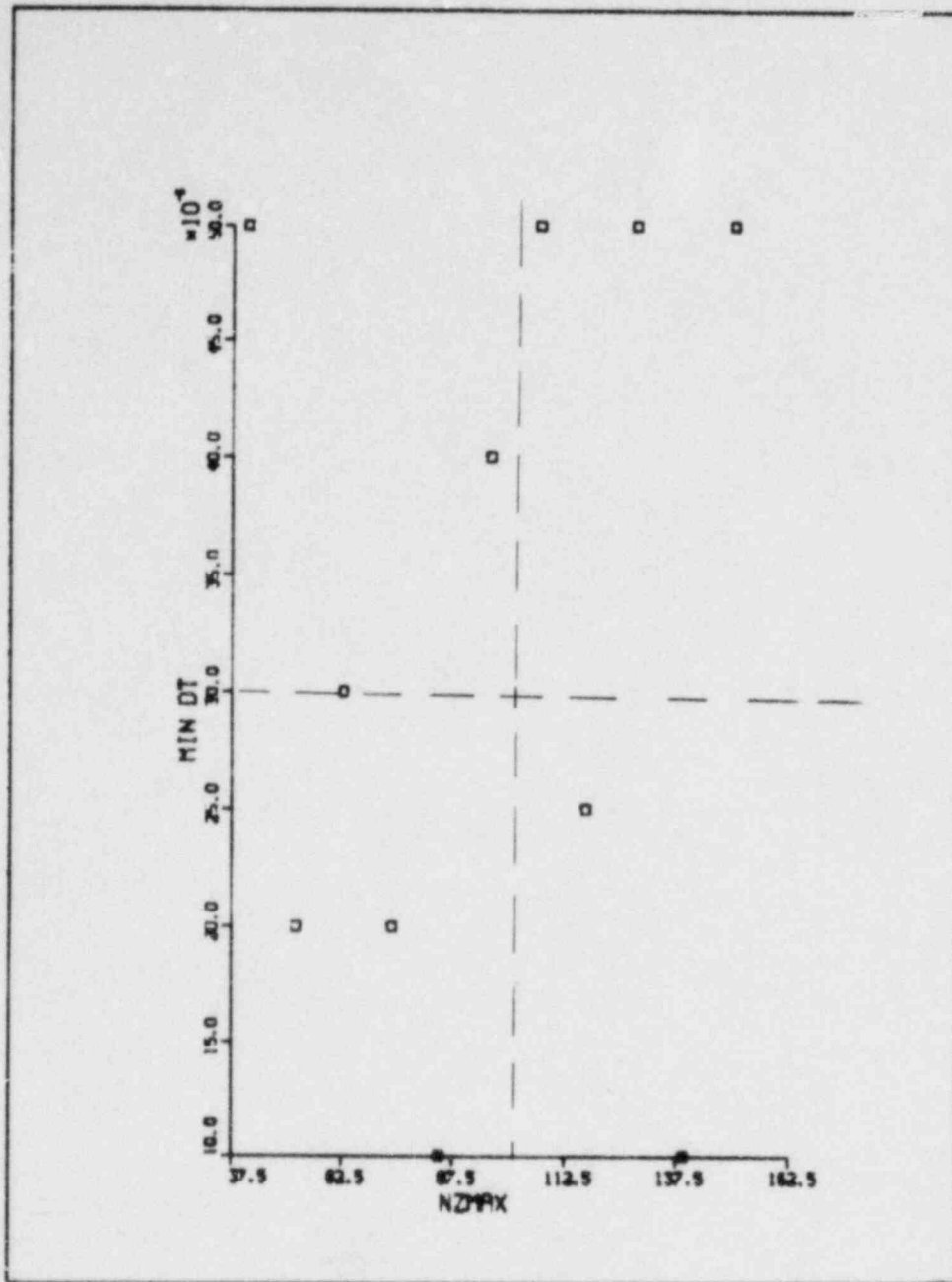


Fig. 31. Minimum time step size as a function of maximum rows of nodes for the conduction calculation.

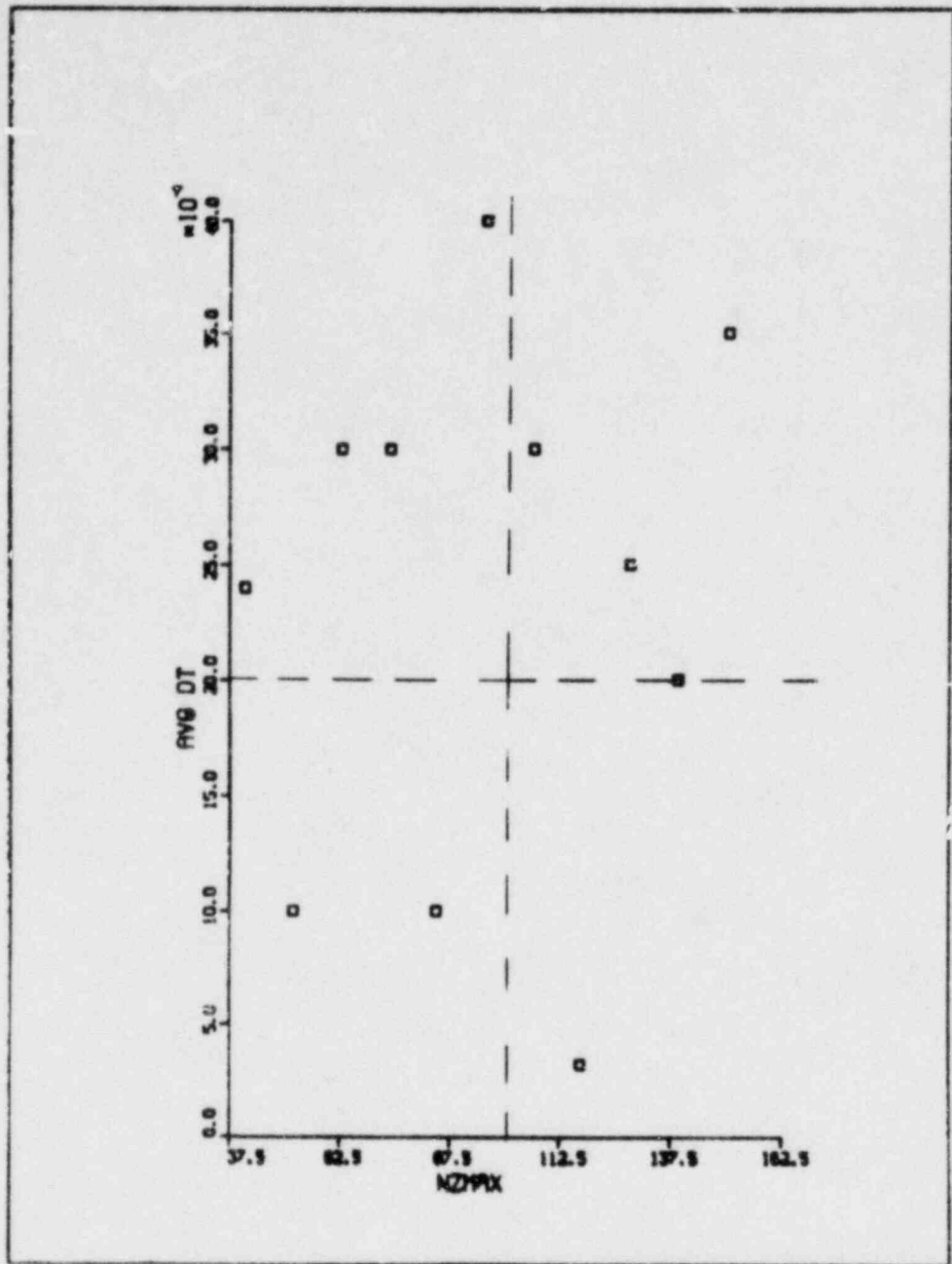


Fig. 32. Average time step size as a function of maximum rows of nodes for the conduction calculation.

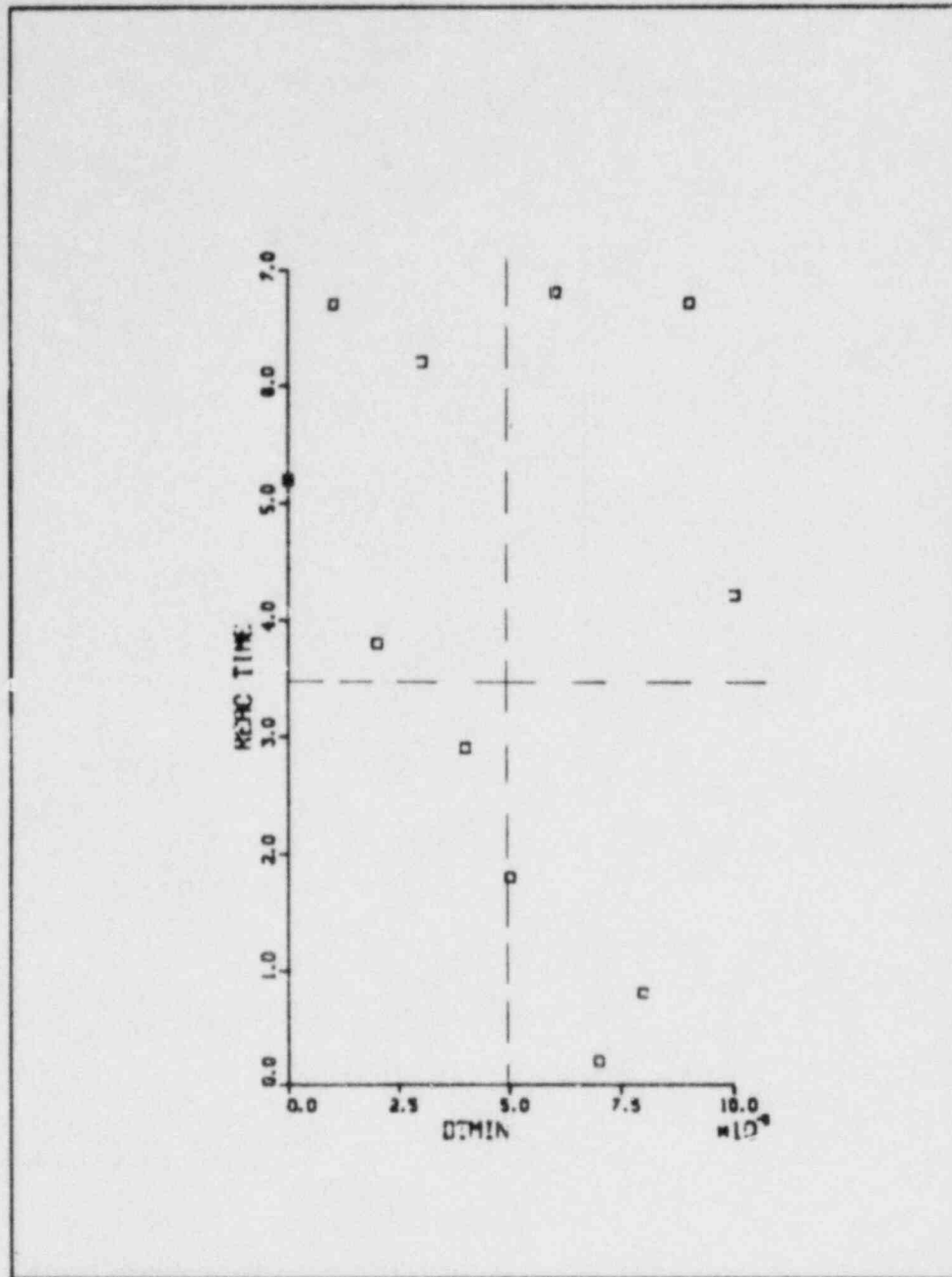


Fig. 33. Reactor time as a function of minimum time step size.

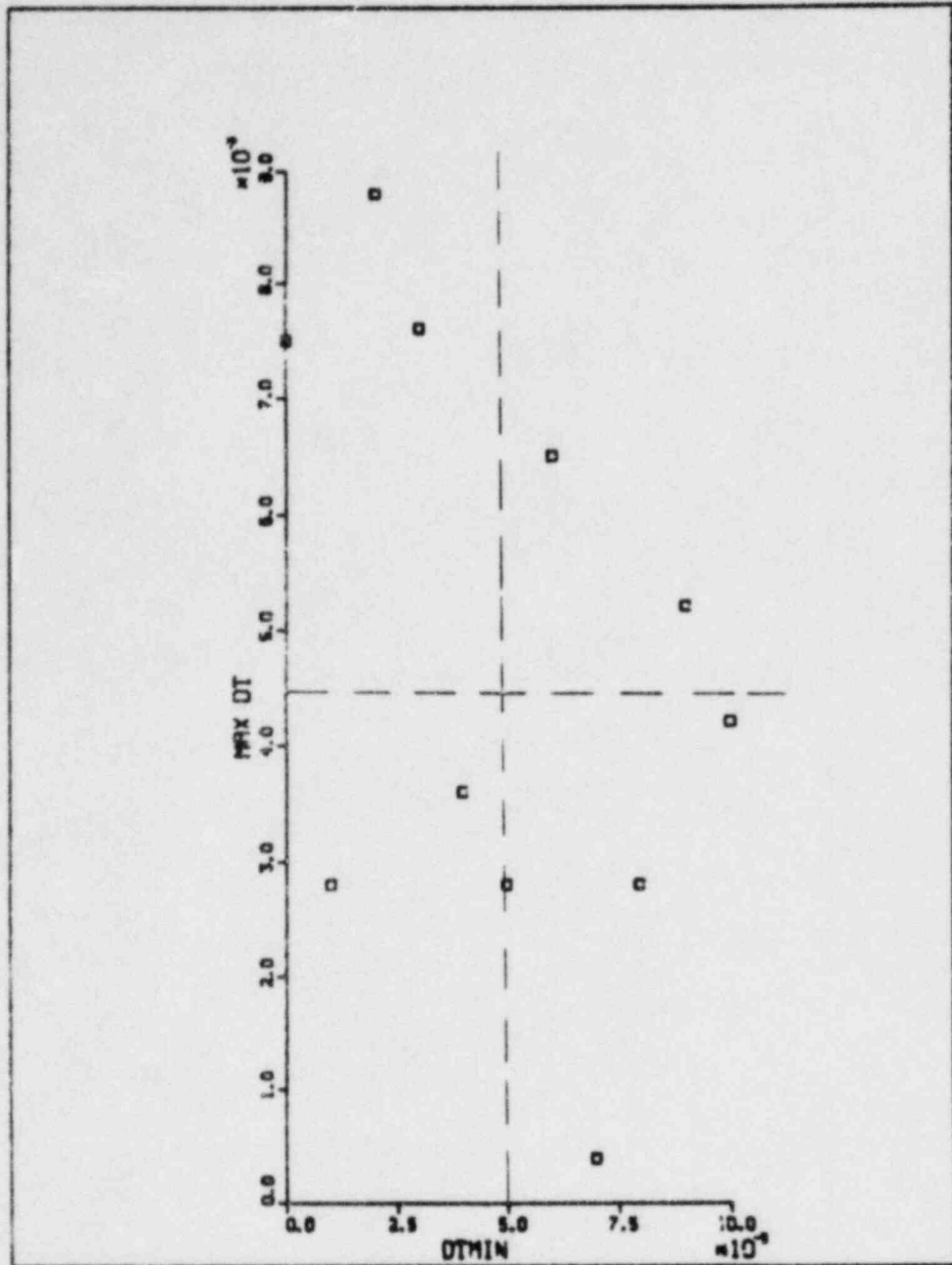


Fig. 34. Maximum time step size as a function of minimum time step size.

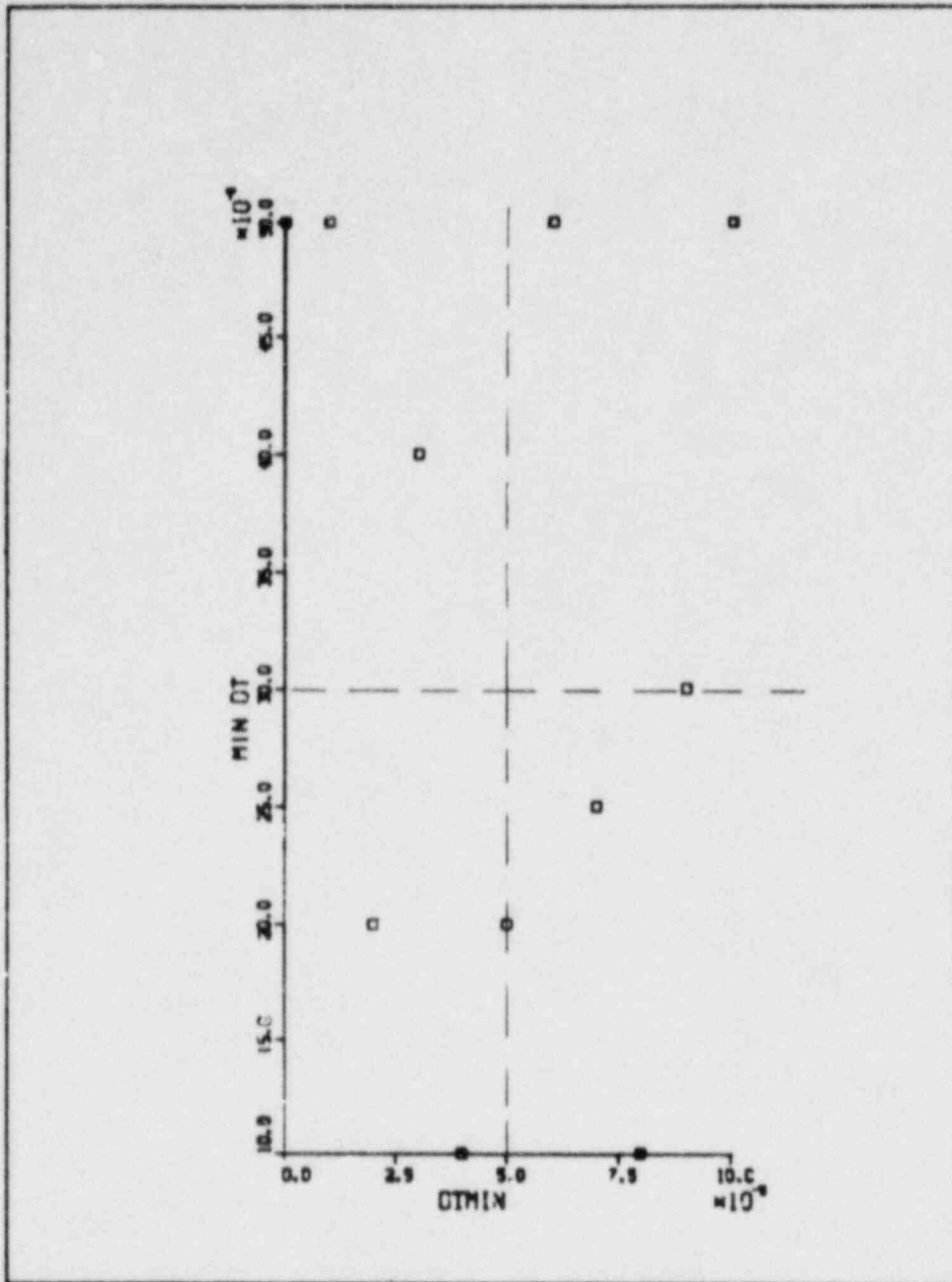


Fig. 35. Minimum time step size as a function of minimum time step size.

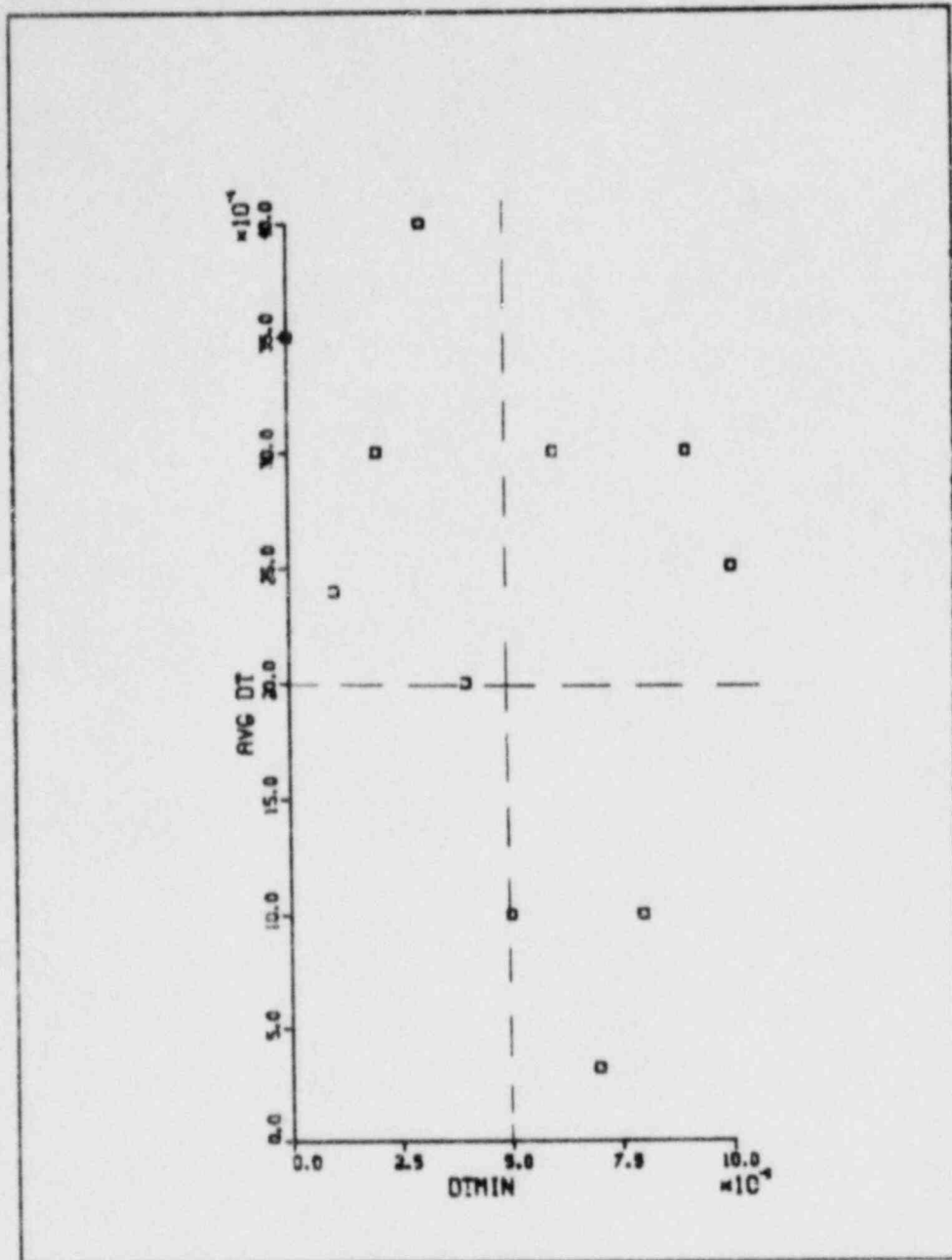


Fig. 36. Average time step size as a function of minimum time step size.

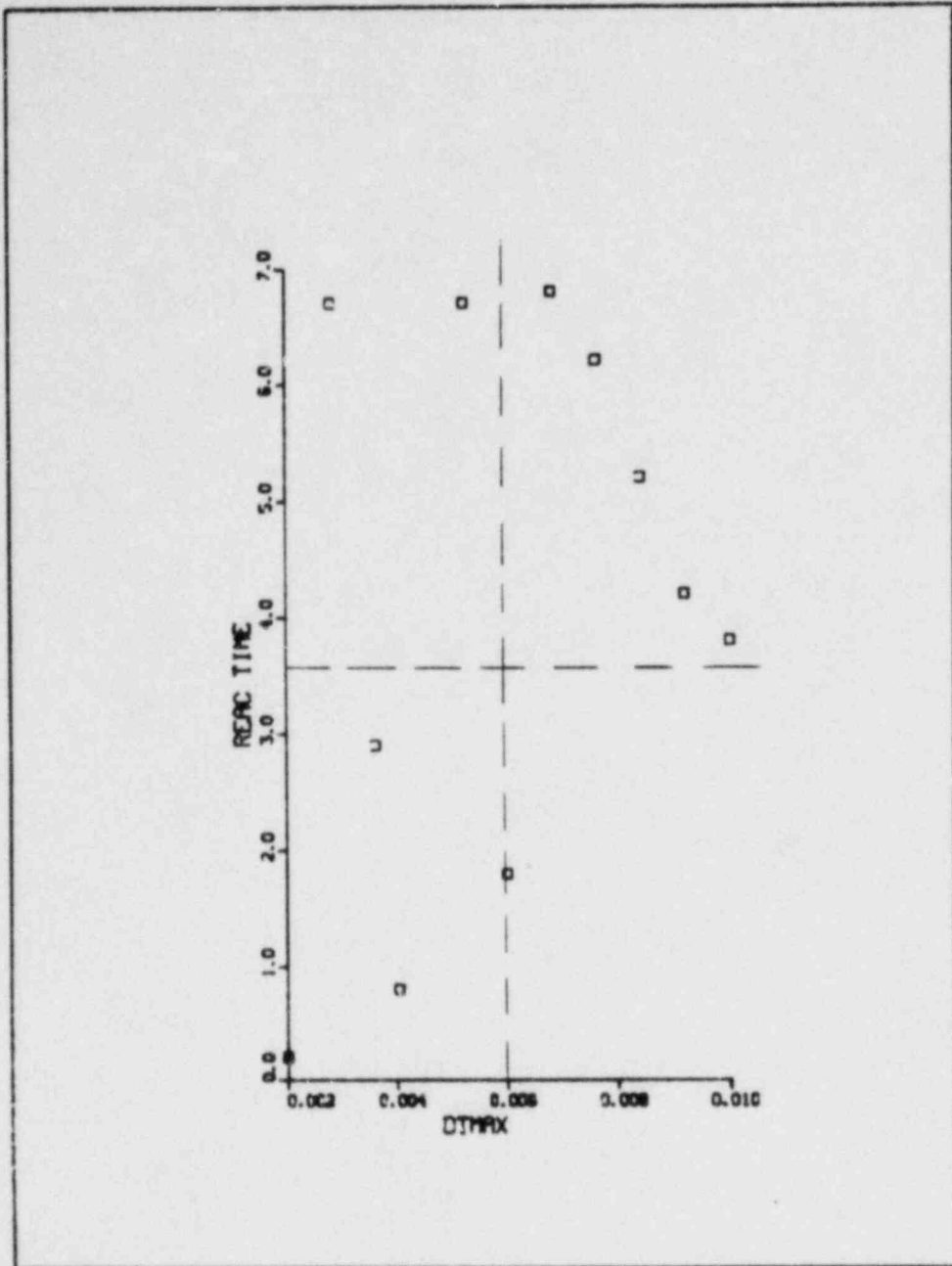


Fig. 37. Reactor time as a function of maximum time step size.

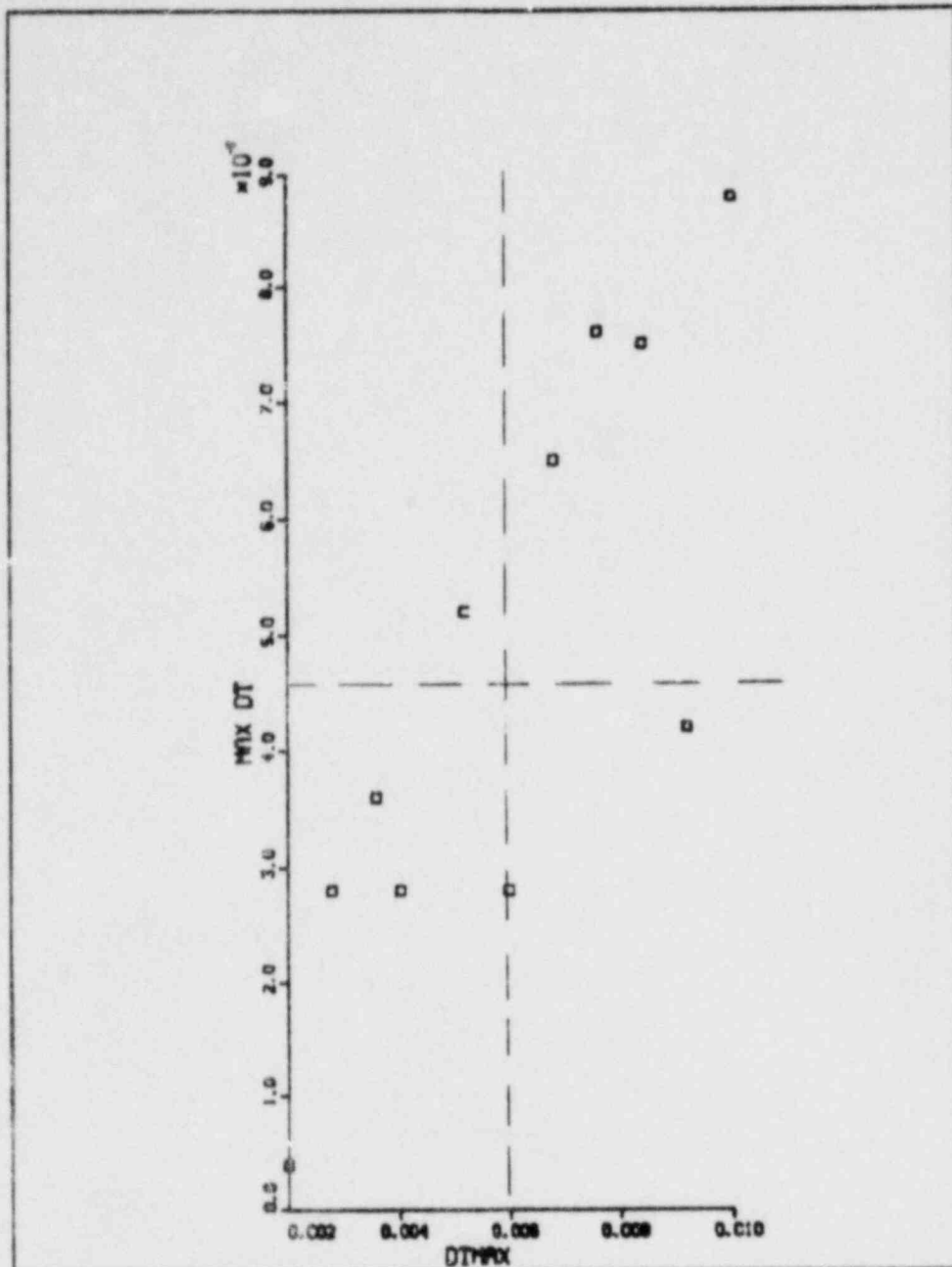


Fig. 38. Maximum time step size as a function of maximum time step size.

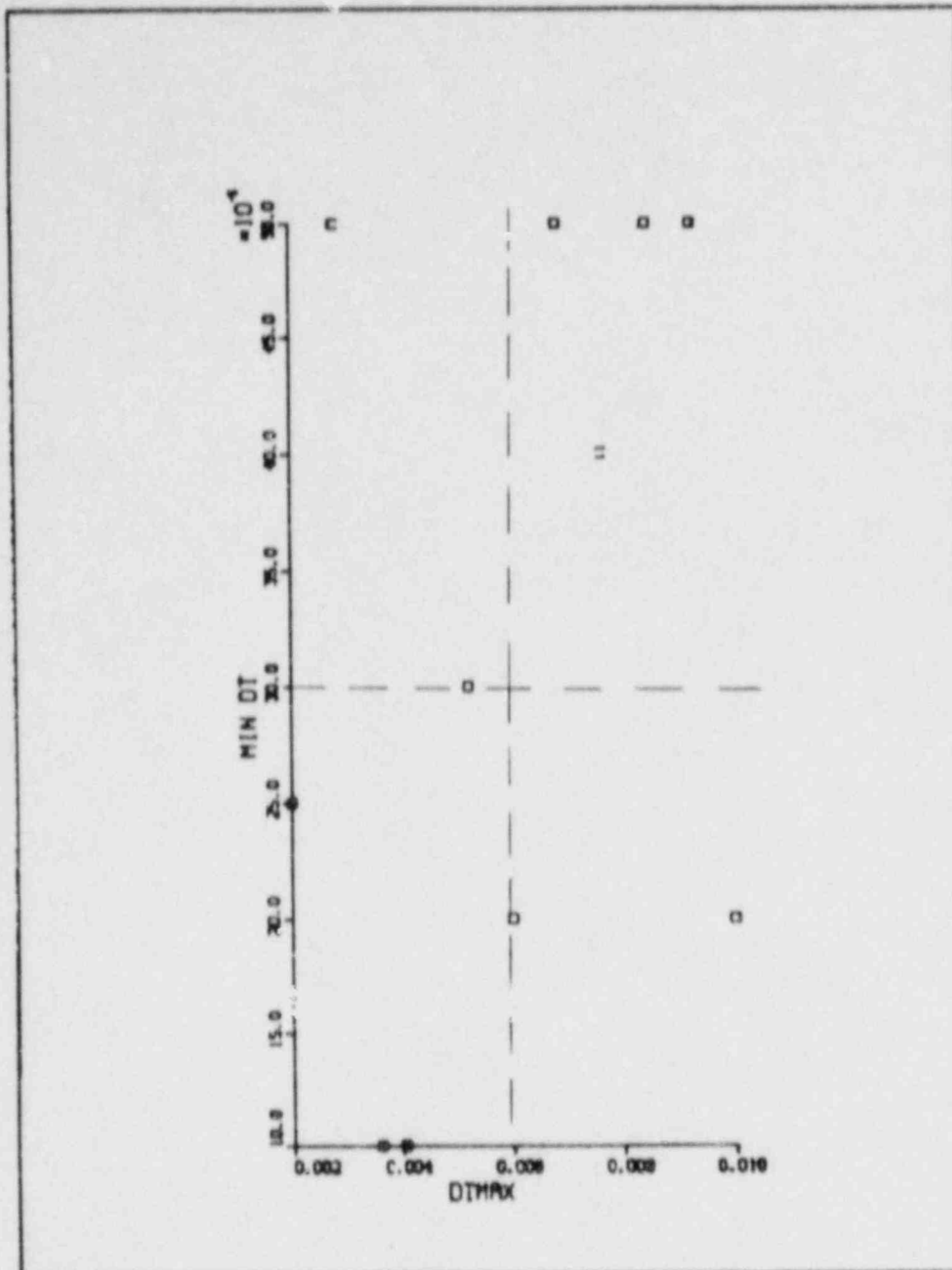


Fig. 39. Minimum time step size as a function of maximum time step size.

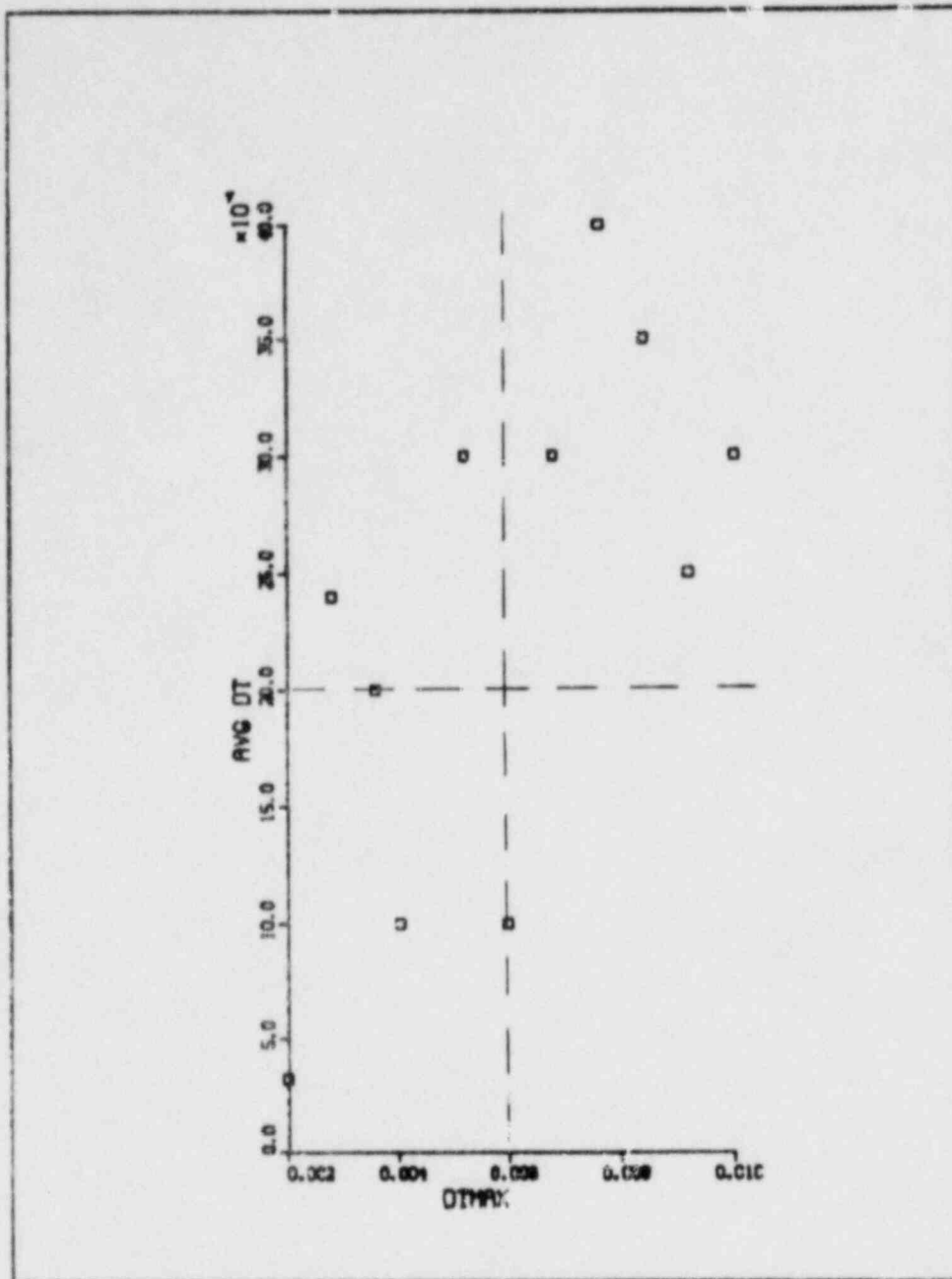


Fig. 40. Average time step size as a function of maximum time step size.

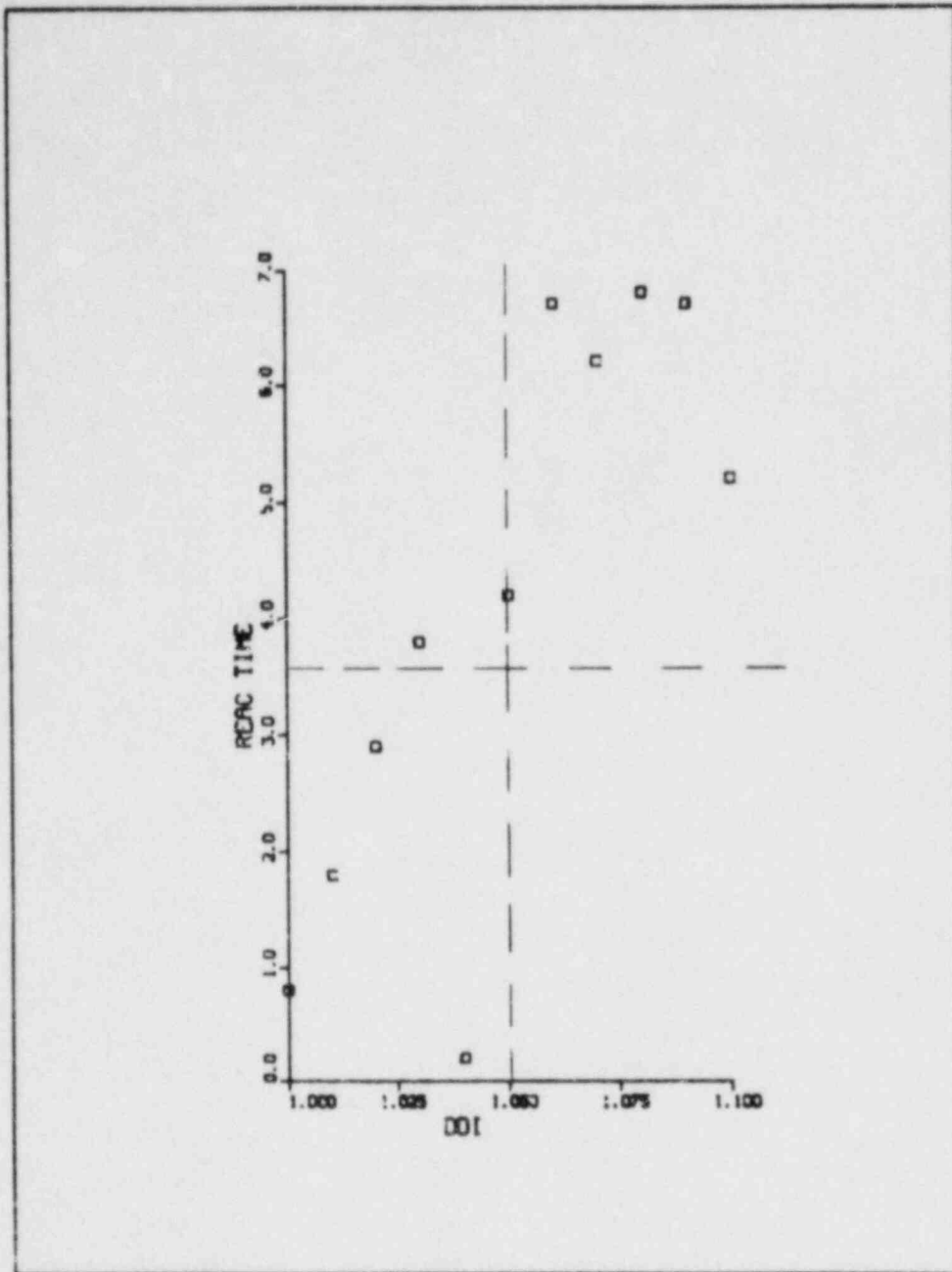


Fig. 41. Reactor time as a function of time step accelerator.

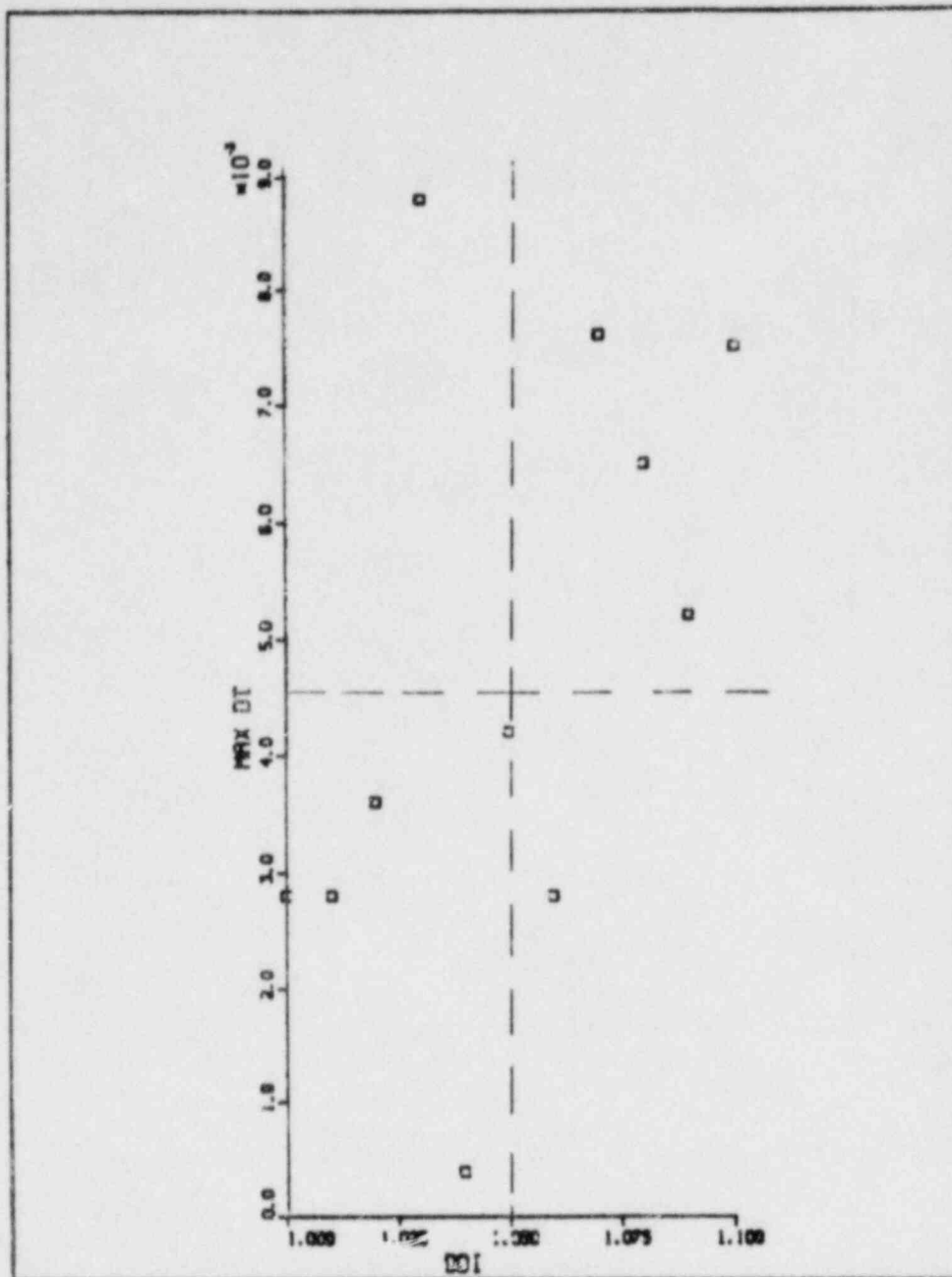


Fig. 42. Maximum time step size as a function of time step accelerator.

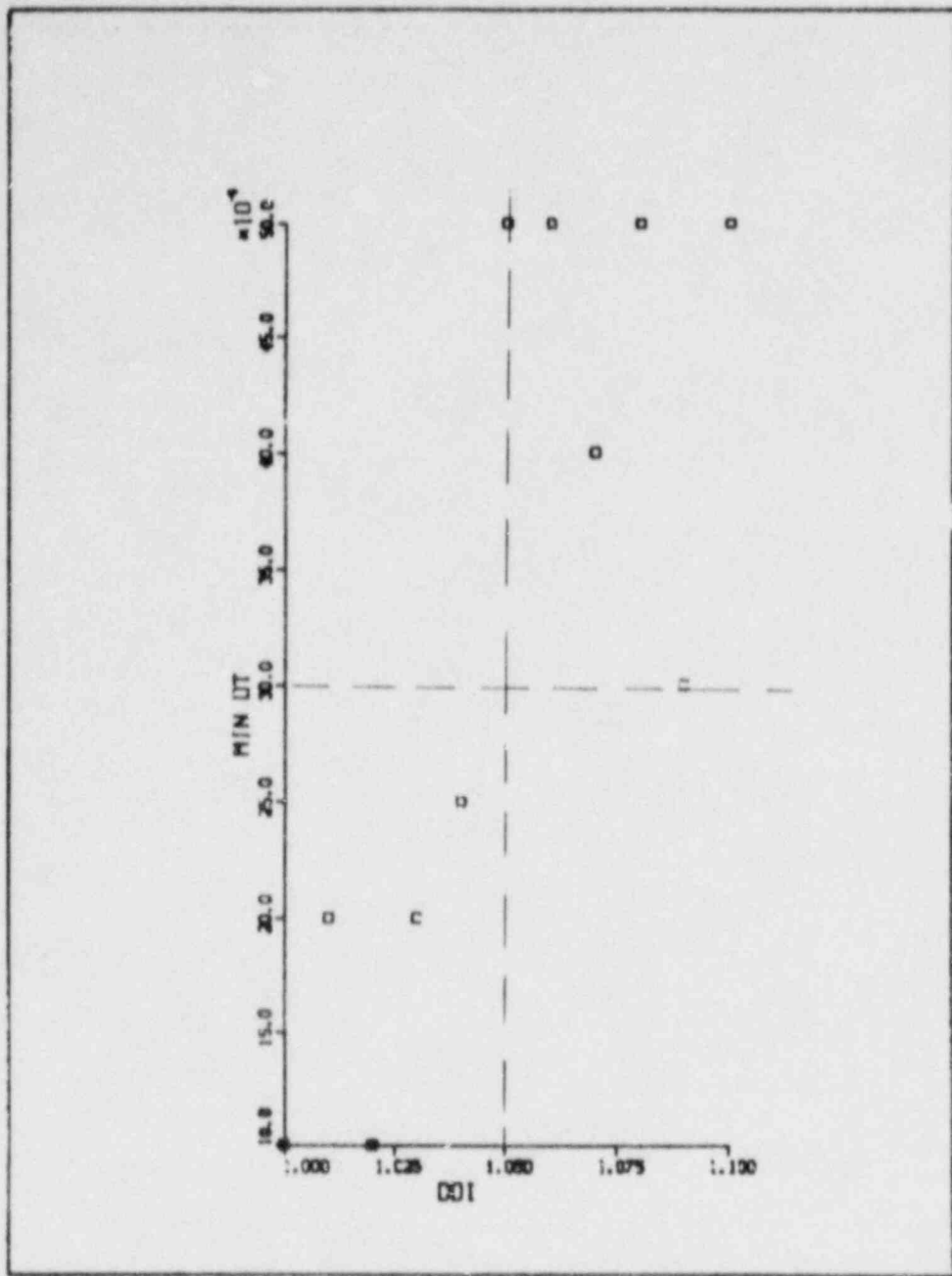


Fig. 43. Minimum time step size as a function of time step accelerator.

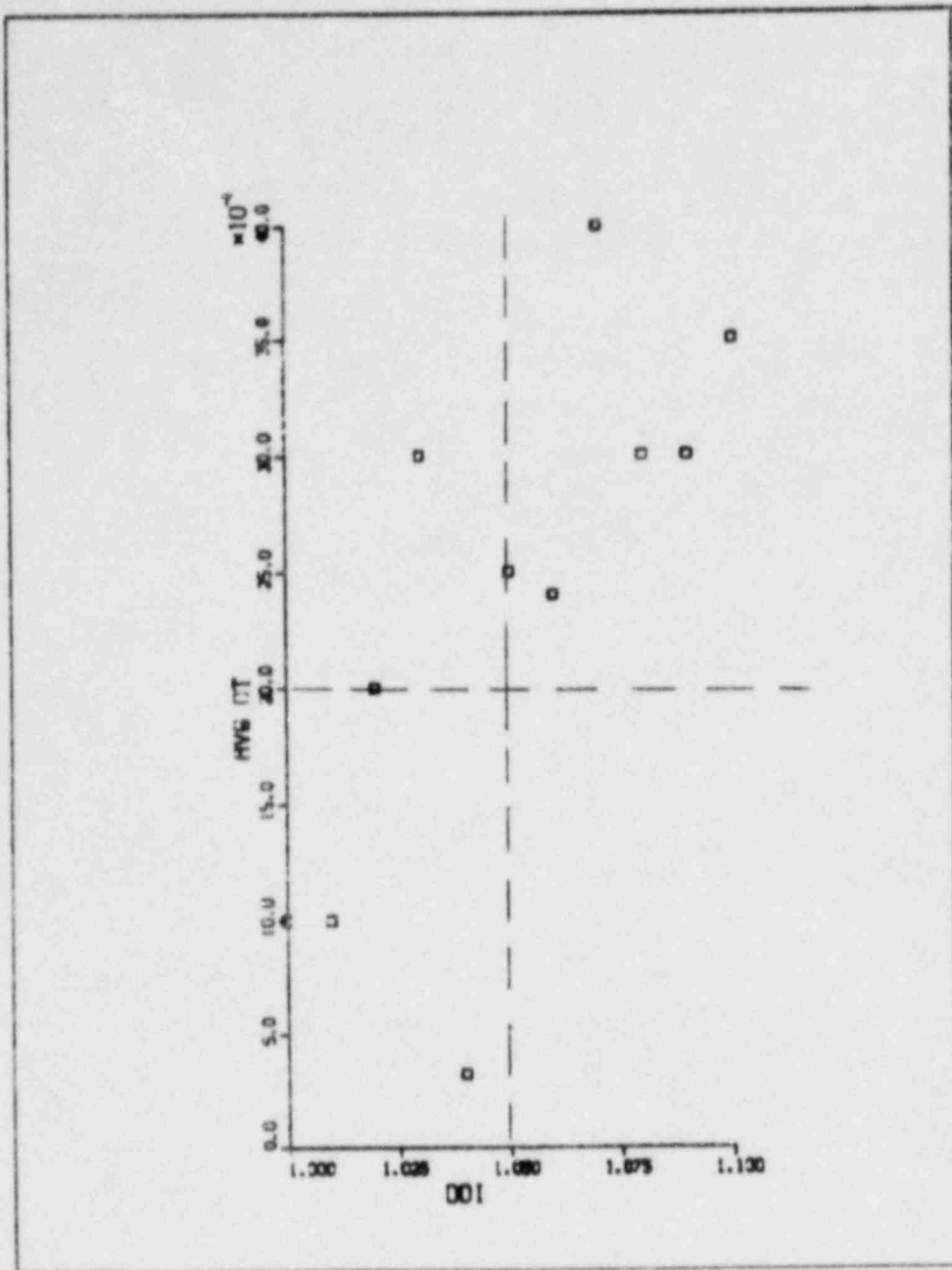


Fig. 44. Average time step size as a function of time step accelerator.

DISTRIBUTION

	<u>Copies</u>
Nuclear Regulatory Commission, R4, Bethesda, Maryland	388
Technical Information Center, Oak Ridge, Tennessee	2
Los Alamos National Laboratory, Los Alamos, New Mexico	<u>50</u>
TOTAL	440

Available from
GPO Sales Program
Division of Technical Information and Document Control
US Nuclear Regulatory Commission
Washington, DC 20555
and
National Technical Information Service
Springfield, VA 22161